

# 1. INTRODUCTION

## 1.1 Background

The largest resources of Platinum Group Elements (PGE's) are found in the Bushveld Complex situated in the central portion of the Transvaal in South Africa. Three reefs varying in mineralogy and ore grade are currently mined for PGE's. These are the Merensky Reef, UG2 and Plat Reef (Viljoen & Schurmann, 1998; Cawthorn, 1999).

Figure 1.1 is a simplified flow diagram is given of a typical route to recover PGE's from these ores. After milling and flotation, the concentrate (which still contains a large fraction of oxides and silicates) is molten in a furnace to produce two immiscible melts. The lighter silicate melt (furnace slag) is tapped continuously and discarded while the heavier sulphide melt (matte) is tapped at regular intervals and further treated (Hiemstra, 1988). This is followed by conversion of the matte (by air or air-oxygen mixes) that involves oxidation of most of the Fe, which then reacts with added SiO<sub>2</sub> to form fayalite (Fe<sub>2</sub>SiO<sub>4</sub>) slag (Mostert & Roberts, 1973). The simultaneous oxidation of sulphur leads to the formation of SO<sub>2</sub> (Cooper, 1984). The converted matte contains Cu, Ni, S and small amounts of Fe and Co as well as trace amounts of PGE's, gold and silver. The conversion process enriches the PGE content in the matte by approximately 3-fold, compared to furnace matte. This matte is poured into large ingots (lined with a refractory material) where it is slow cooled over a period of approximately 5 days. Depending on the bulk composition and temperature, the matte crystallizes slowly according to a specific path of crystallization. Ideally, a magnetic alloy fraction will crystallize first from the matte and act as collectors of most of the PGE's.

Platinum Group Elements have a preferred partitioning into an alloy phase compared to sulphide or oxide phases (Distler et al., 1977; Fleet & Stone, 1991; Peach & Mathez, 1996, Crocket et al., 1997; Fleet et al., 1999). In this case the PGE's will be captured by a crystallizing Cu-Ni-alloy. The fully crystallized matte is then milled and magnetically separated to remove the now PGE-concentrated alloy fraction from the sulphide fraction (Mostert & Roberts, 1973; Schouwstra et al., 1998). This PGE-concentrate is further treated chemically to separate and concentrate the different Platinum Group Elements.

For this study the key step in the process is the slow cooling of the matte that will both save time and money by reducing the amount of material that must be chemically treated to unlock the PGE's. To ensure an optimum recovery of the PGE's, the starting composition and temperature of the matte must be within calculated limits to regulate the path of crystallization (Mostert & Roberts, 1973; Bruwer & Merkle, 1998 and Jones, 1999).

## 1.2 Aim of Study

The setting for this study is the pyrometallurgical processes in the beneficiation of platinum group elements from a Cu-Ni-Fe-sulphide ore. To understand the relevancy of the Cu-Ni-Fe-S system in the beneficiation of PGE's, a short summary of the processes involved in treatment of the ore are given in Figure 1.1.

The aim of the study is to investigate the influence of low concentrations of Fe on the Cu-Ni-S system. Of particular interest are: (1) the compositions of the alloy and digenite co-existing with melt (generally referred to as the cotectic alloy, cotectic digenite and cotectic melt) in the different isothermal sections; (2) the Fe content of sulphide and alloy phases as a function of the Fe to the starting composition, and (3) the partitioning of Fe between co-existing solid phases. The focus is not to present complete phase diagrams, and some phase diagrams will appear incomplete in areas of less relevancy to this project.

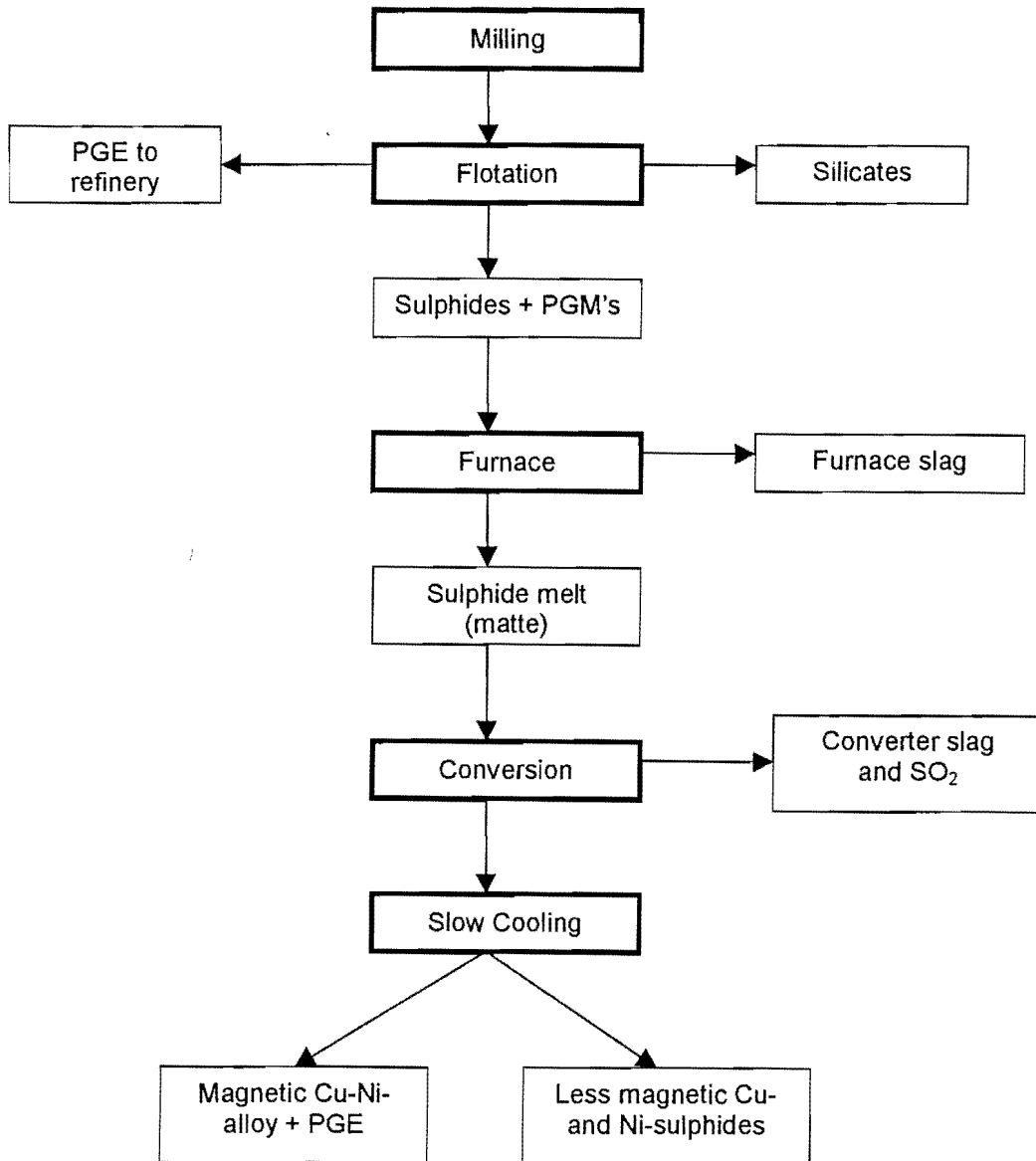
After conversion, the relevant Cu-Ni-matte (at the plant) contains approximately 3 wt% Fe. However, to determine the influence of Fe on the Cu-Ni-S system it was decided to perform experiments at lower (1 wt%), higher (5 wt%) and much higher (10 wt%) concentrations of Fe, than in the average matte. The percentage Ni is approximately 50%, Cu approximately 28% and sulphur approximately 21% (Hiemstra, 1988, Mostert & Roberts, 1973 and Jones, 1999). Bruwer and Merkle (1998) demonstrated that at low Fe contents the crystallization paths of converter mattes are very sensitive to the amount of sulphur present.

A prerequisite for understanding the crystallization paths of a slow-cooled matte is the phase diagrams for the system Cu-Ni-Fe-S as an approximation of converter matte composition. Available information includes phase diagrams of the sub-systems and their applications to natural occurring systems (see Chapter 2). To predict and optimize the conditions necessary for a converter matte to collect PGM's in an extractable fraction, the characteristics of the Cu-Ni-Fe-S system needed to be investigated experimentally.

To assure the direct relevancy of this project to the beneficiation of Cu, Ni and PGE's from a Merensky Reef and UG2-type Cu-Ni-PGE ore, some constraints were put on the parameters for the investigation. The temperature range was confined to 700° - 1200°C at 100°C intervals and the Fe content was set at 1, 3, 5, and 10wt% Fe. The starting temperature of a converter matte is normally in the vicinity of 1200°C, where only alloy phases are stable. At lower temperatures sulphide phases would become stable, competing with the alloy phases for incorporating the PGE's. Higher experimental temperatures than 1200°C were not needed because there would not be any additional phases in the pure Cu-Ni-Fe-S system. Decreasing the experimental temperatures in 100°C intervals were small enough steps to detect any important change of phase relations in the system. Experiments were not performed below 700°C for two reasons: Firstly, equilibration times at these low temperatures

become very long (possibly 6 to 12 months) and would carry on beyond the time restrictions of this study. Secondly, at 700°C most of the PGE's in the matte would have been collected by the alloy and sulphide phases.

**Figure 1.1: Simplified flow diagram showing the route of slow cooling for PGM beneficiation from a Merensky Reef and UG2-type sulphide ore.**



## 2. UNDERLYING BINARY AND TERNARY SYSTEMS AND THEIR PHASES

Experimental studies on various natural and synthetic systems were performed extensively in the late fifties, sixties and seventies (see below). Although much can be derived from thermodynamic predictions, the actual experiment is still the most reliable method to determine the properties of an investigated system.

Ores and natural mineral assemblages have rather been described by the sub-systems than the complete Cu-Ni-Fe-S system. Summarized below are the relevant binary and ternary systems as been discussed by researchers over the years.

### 2.1 The Ni-S system

Minerals occurring in the Ni-S system were experimentally investigated and described by Arnold and Kullerud (1956) and Kullerud and Yund (1962). Arnold and Kullerud (1956) described the NiS-NiS<sub>2</sub> join to be a solid solution of the omission type and suggested a formula of Ni<sub>1-x</sub>S. A follow-up study (Kullerud and Yund, 1962) with the use of quenched experiments in evacuated quartz glass tubes, DTA, and high-temperature X-ray powder diffraction extended on the phases present in the system. Ni-sulphides relevant for this study are:

#### *2.1.1) Heazlewoodite (Ni<sub>3</sub>S<sub>2</sub>)*

Heazlewoodite occurs as two modifications with the inversion temperature at 555° ± 5°C (Rosenqvist, 1954). The low temperature polymorph has a hexagonal (rhombohedral) structure and limited solid solution on either side of the stoichiometric Ni<sub>3</sub>S<sub>2</sub>. The high-temperature form shows a compositional variation from 24.0 to 30.0 wt% S between 600° and 700°C, resulting in a general formula of Ni<sub>3±x</sub>S<sub>2</sub>. Sinyakova et al. (1999) determined through an experimental investigation that heazlewoodite-solid-solution forms between 875°C and 880°C

#### *2.1.2) Millerite (NiS)*

Millerite also has a low-temperature hexagonal form (β) that inverts to a high-temperature hexagonal (NiAs atomic structure) polymorph (α) at 379° ± 3°C (Alsen, 1923, 1925; Kullerud & Yund, 1962). At a temperature of 600°C, the high-temperature form can contain a maximum of 37.8 wt% S (Arnold & Kullerud, 1956). According to the investigation of Arnold and Kullerud (1956), the β-millerite often occurs in long needle-shaped crystals whereas the α-millerite seldomly occurs as single crystals. In the temperature range 700° - 800°C, the α-NiS inverts

to  $\alpha$ -Ni<sub>1-x</sub>S. The melting point, as determined by Eugster and Kullerud (1956), is  $800.5^{\circ}\pm 1.0^{\circ}\text{C}$ .

### 2.1.3) Polydymite (Ni<sub>3</sub>S<sub>4</sub>)

A diagnostic characteristic of polydymite is polysynthetic twinning and the replacement of Ni by Fe to form (Ni, Fe)<sub>3</sub>S<sub>4</sub> in natural systems (Tarr, 1935). Polydymite forms part of the linnaeite (Co<sub>3</sub>S<sub>4</sub>) series together with violarite (Ni<sub>2</sub>FeS<sub>4</sub>) (Palache et al., 1944). Kullerud and Yund (1962) found that the synthesis of polydymite was hampered by slow reaction rates. Other compounds (like Ni<sub>7</sub>S<sub>6</sub>, Ni<sub>1-x</sub>S, and NiS<sub>2</sub>) that grow at the same time will grow faster and persist longer metastably. According to Rosenqvist (1954), polydymite was not observed in experiments at 400°C. Therefore, the chances of encountering this phase are very remote.

### 2.1.4) Vaesite (NiS<sub>2</sub>)

Vaesite has the pyrite structure and was synthesized from 170° to 680°C (De Jong & Willems, 1927; Lundqvist, 1947). To synthesize vaesite requires the formation of NiS first and long reaction times. Vaesite is stoichiometric within the limits of NiS<sub>2.000±0.0004</sub> according to Kullerud and Yund (1962).

## 2.2 The Cu-S system

The Cu-S system was investigated by Roseboom (1966) at temperatures between 25° and 700°C. The thermochemical properties were investigated by Kellogg (1967) between 526.75° and 1326.75°C and thermodynamic data are summarized by Chakrabarti and Laughlin (1983). The relevant minerals in this system are:

### 2.2.1) Digenite (Cu<sub>2</sub>S)

At temperatures between 76° and 83°C low-digenite is inverted to high-digenite. The inversion temperature of high-digenite to high-chalcocite is not well defined, but these two minerals are considered equivalent (Roseboom, 1966). At the temperatures relevant for this study high-digenite is considered stable.

### 2.2.2) Covellite (CuS)

Kullerud (1965) described the stability relations of covellite and determined that it breaks down to high-digenite plus liquid sulphur at 507°C. The mineral named blaubleibender covellite was first described by Moh (1964) and again noted by Barton (1973) but not determined to be a stable phase. Later this "mineral" was described and identified to be yarrowite and spionkopite by Goble (1980).

### 2.3 The Fe-S system

Kullerud and Yoder (1959) investigated the stability of pyrite in the Fe-S system and the pyrite-pyrrhotite relationship was briefly discussed by Arnold (1956). However, because of the low concentrations of Fe used in this experimental investigation, no distinct Fe-sulphide phases were observed, and a further discussion on mineral phases in this system is not relevant.

### 2.4 The Ni-Fe-S system

This element combination results in minerals like pentlandite and pyrrhotite that are important ore minerals in natural PGE producing systems. One of the first papers discussing the Ni-Fe-S system was by Hawley et al. in 1943, in which they also describe the solid solution between pyrrhotite and pentlandite.

Describing the subsolidus phase relations in the Ni-Fe-S system, Kullerud (1956) found that the solubility of NiS in FeS at 500°C is about 20 mol% and the solubility of FeS in NiS is about 30 mol%. The solubilities of both sides increase markedly with increasing temperature.

The sulphur-rich portion of the Ni-Fe-S system was investigated between 100° and 1000°C by Clark and Kullerud (1963). Experiments were performed with special emphasis on the pyrite-vaesite join. It was found that the solubility of Fe in NiS<sub>2</sub> (vaesite) and Ni in pyrite is less than 10 % at 550°C, even though vaesite and pyrite are isostructural.

The central portion of the Ni-Fe-S system was discussed between 250° and 600°C by Naldrett, Craig and Kullerud (1967).

A recent investigation in the Fe-Ni-S system by Sinyakova et al. (1999), experimentally determined the surface of the liquidus at low sulphur contents as well as the fields of the monosulphide-solid-solution, heazlewoodite-solid-solution and tenite primary crystallization.

None of the distinct Fe- or Ni-Fe-minerals was observed in this investigation due to the low Fe concentrations used.

### 2.5 The Cu-Fe-S system

Merwin and Lombard (1937) performed an extensive study on the phase relations in the Cu-Fe-S system between 400° and 950°C, while Yund and Kullerud (1966) evaluated the thermal stabilities of assemblages in this system from 700° to 200°C. Crystal-chemical studies were performed by Morimoto in 1970.

Rooseboom and Kullerud (1958) investigated the solidus in the sulphur rich part of this system between 400° and 800°C, and found that digenite and bornite form a complete solid solution in the presence of liquid and vapor above 550°C. This was confirmed by Barton (1973), who investigated the solid solutions in the Cu-Fe-S system and determined the activities of digenite, chalcocite and  $\text{CuFeS}_2$ . He also present a phase diagram for the Cu-Fe-S join between 400° and 700°C. Cabri (1973) described and attempted to synthesize the phases in this system at lower temperatures (100° and 600°C).

## 2.6 The Cu-Ni-S system

The bulk of this investigation expands on the experimental study performed by Bruwer (1996) on the Cu-Ni-S system between 700°C and 1200°C (at 100°C intervals). With the low Fe contents researched in this study, the similarities and differences with the Fe-free system are important aspects. The phase diagrams produced by Bruwer (1996) of the Cu-Ni-S system will therefore be briefly discussed at the different isothermal sections, presuming cooling from higher temperature. Stable assemblages are presented in brackets.

### *2.6.1) At 1200°C*

Two immiscible melts coexist at Cu-rich compositions of the system and at Ni-rich compositions a (alloy + melt)-field extends towards higher Cu contents. The position of intersection of the (alloy + melt)-field boundary line with the Cu-Ni join is at approximately 80 wt% Cu and with the Ni-S join at approximately 23 wt% Ni (Figure 2.1).

### *2.6.2) At 1100°C*

Two immiscible melts coexist at Cu-rich compositions of the system and at Ni-rich compositions a (alloy + melt)-field extends towards higher Cu contents but flattens out at about 95 wt% Cu. The position of intersection of the (alloy + melt)-field boundary line with the Cu-Ni join is at approximately 95 wt% Cu and with the Ni-S join at approximately 30 wt% Ni (Figure 2.2).

### *2.6.3) At 1000°C*

At Cu-rich compositions and less than 20 wt% S, digenite and alloy co-exist. At Ni-rich compositions alloy and melt co-exist with the (alloy + melt)-field boundary line intersecting the Ni-S join at approximately 18 wt% S. At more than 50 wt% Cu, low Ni contents, and not more than 20 wt% S, three phases co-exist: alloy, digenite and melt. At higher sulphur contents (about 20 wt%), digenite and melt co-exist (Figure 2.3).

#### 2.6.4) At 900°C

At Cu-rich compositions and less than 20 wt% S, digenite and alloy co-exist. At Ni-rich compositions alloy and melt co-exist with the (alloy + melt)-field boundary line intersecting the Ni-S join at approximately 20 wt% S. At more than 40 wt% Cu, up to 50 wt% Ni, and not more than 20 wt% S, three phases co-exist: alloy, digenite and melt. At higher sulphur contents (between 20 and 25 wt%), digenite and melt co-exist. At high Ni concentrations and less than 50 wt% S, millerite and vaesite both co-exist with a melt. Less melt is present than at higher temperatures (Figure 2.4).

#### 2.6.5) At 800°C

All the solid phases co-exist with melts and some also co-exist only with each other as the quantity of melt decrease. At Cu-rich compositions and less than 20 wt% S, digenite and alloy co-exist. At Ni-rich compositions alloy and melt co-exist with the (alloy + melt)-field boundary line intersecting the Ni-S join at approximately 21 wt% S. At more than 20 wt% Cu, up to 60 wt% Ni and not more than 20 wt% S, three phases co-exist: alloy, digenite and melt. At higher sulphur contents (between 20 and 30 wt%), digenite and melt co-exist. At high Ni concentrations and less than ~50 wt% S, millerite and vaesite co-exist each with a different melt. Heazlewoodite is stable at this temperature (Figure 2.5).

#### 2.6.6) At 700°C

Only digenite, a Ni-rich alloy and heazlewoodite still co-exist with a melt phase. Millerite and vaesite co-exist only with each other and digenite. Only a very small amount of melt is left (Figure 2.6).

### 2.7 The Cu-Ni-Fe-S system

Kullerud et al. (1969) investigated the phase relations in the three subsystems Cu-Fe-S, Cu-Ni-S and Fe-Ni-S with the silica-tube quenching technique, DTA and high-temperature XRD experiments. They found that extensive liquid immiscibility fields span the sulphur-rich region of all three of the systems while a homogeneous liquid field dominates the central portions of the system. Craig and Kullerud (1969) presented phase diagrams at 1000°C and 850°C of the Cu-Ni-Fe-S system (Figures 2.7 and 2.8), based on experimental work. These phase diagrams were however, drawn without quantitative data and are considered schematic only.

The fractional crystallization of a sulphide liquid in the Fe-Ni-Cu-S system was discussed by Fleet & Pan (1994) at 50 and 52.5 at% S, temperatures between 850 – 1050°C and low pressures. They found that an intermediate solid solution [(Cu,Fe)S<sub>1-x</sub>; iss] is stable up to 900-



950°C in Ni-poor compositions, and a large field of a ternary (Fe,Cu,Ni)S solid solution exists at and below 850°C.

An experimental investigation by Ebel and Naldrett (1996 & 1997) looked at the fractional crystallization of sulphide ores at temperatures between 1050° and 1180°C. Partitioning coefficients for Cu and Ni between monosulphide solid solution and a Fe-Ni-Cu-S liquid are also discussed. Because the study by Ebel and Naldrett looked at high Fe contents the relevancy to this investigation was very limited. A schematic quaternary diagram (Figure 2.9) at 1100°C shows the position of various solid solutions discussed by Ebel and Naldrett (1997). Electron microprobe data is published but their investigation concentrated on the Fe "saturated" part of the quaternary. A similar study by Ballhaus et al. (2001) looked at the role of the metal/S atomic ratio on monosulphide-melt partition coefficients and closed-system fractionation paths in the Fe-Ni-Cu-S system.

Using parameters from the binaries, Kongoli et al. (1998) constructed a modified quasichemical model that predicts the thermodynamic properties of amongst others Fe-Ni-Cu-S mattes over wide range of compositions and temperatures. These model parameters are stored in the databases of the F\*A\*C\*T (1995) thermodynamic computer system, but not utilized (due to costs) in this study.

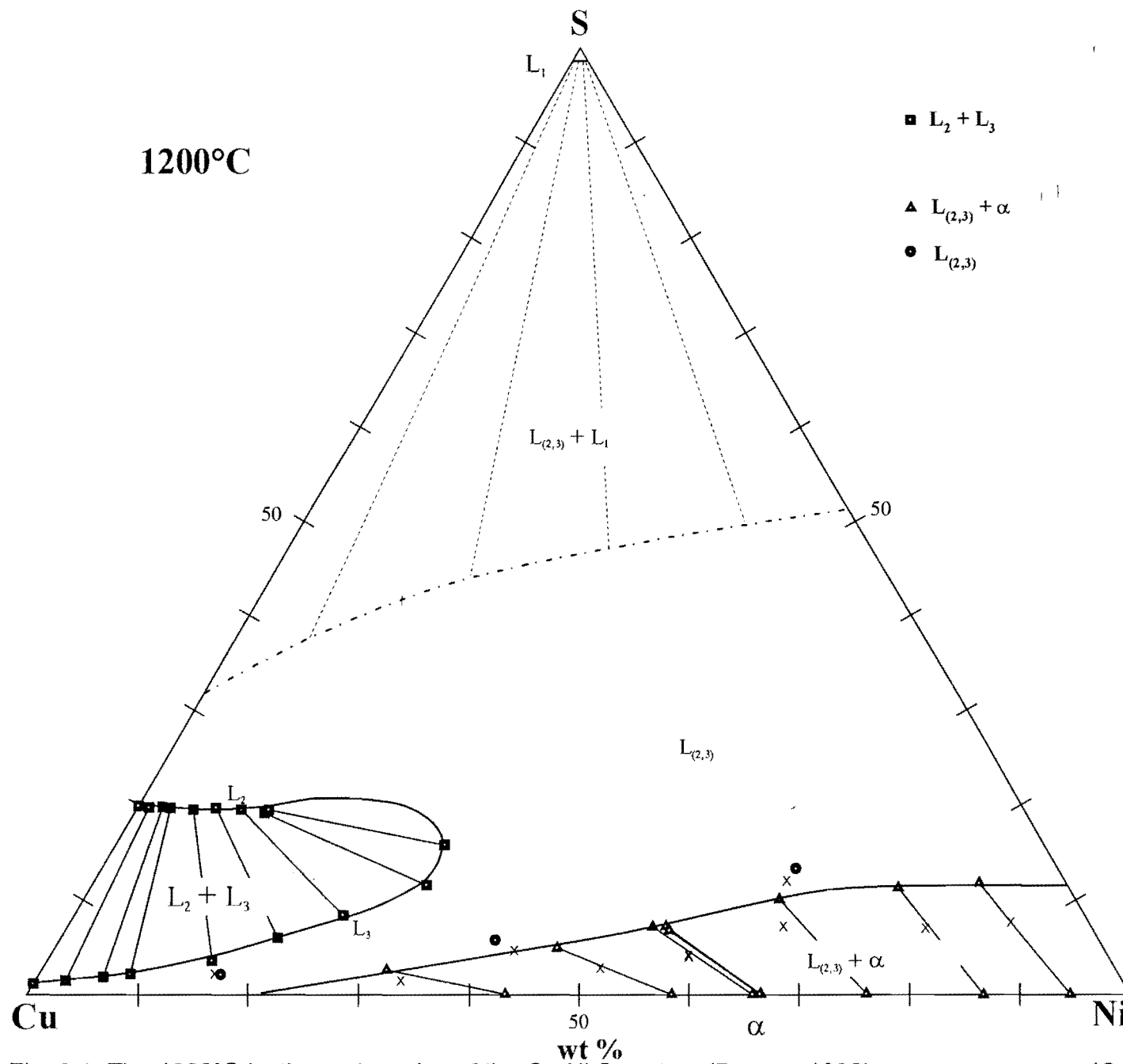


Fig. 2.1: The 1200°C isothermal section of the Cu-Ni-S system (Bruwer, 1996).

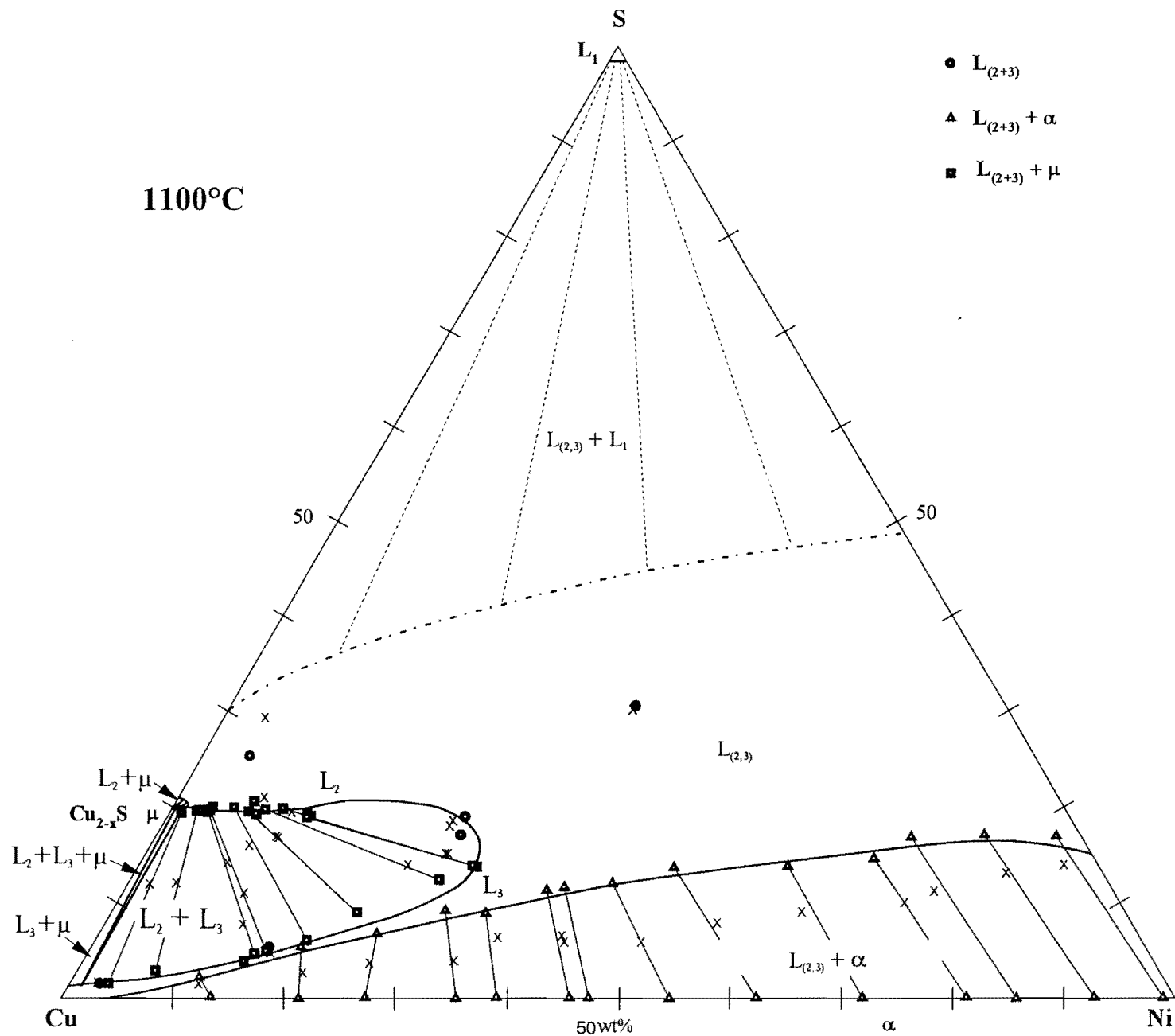


Fig. 2.2: The 1100°C isothermal section of the Cu-Ni-S system (Bruwer, 1996).

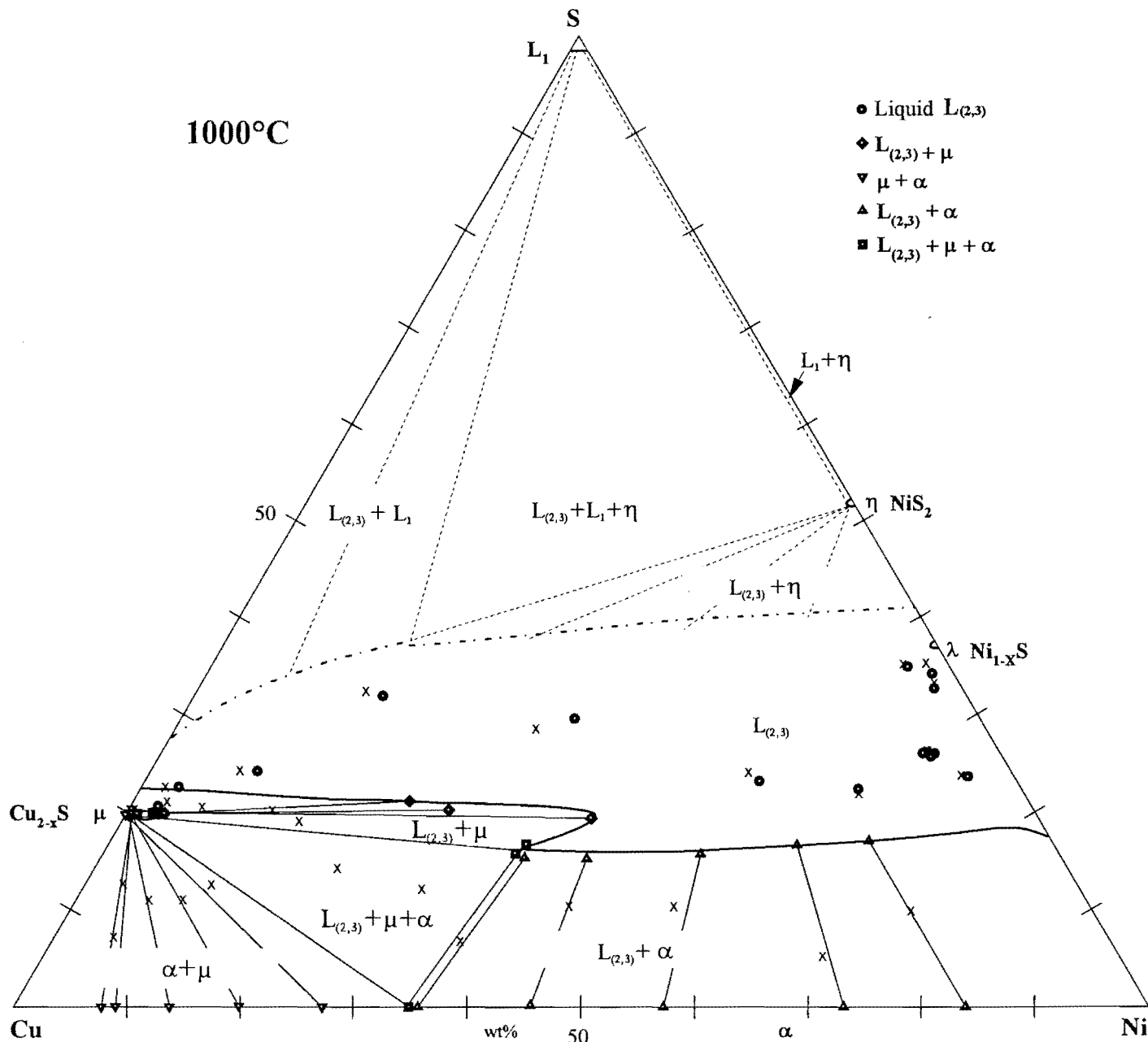


Fig. 2.3: The 1000°C isothermal section of the Cu-Ni-S system (Bruwer, 1996).

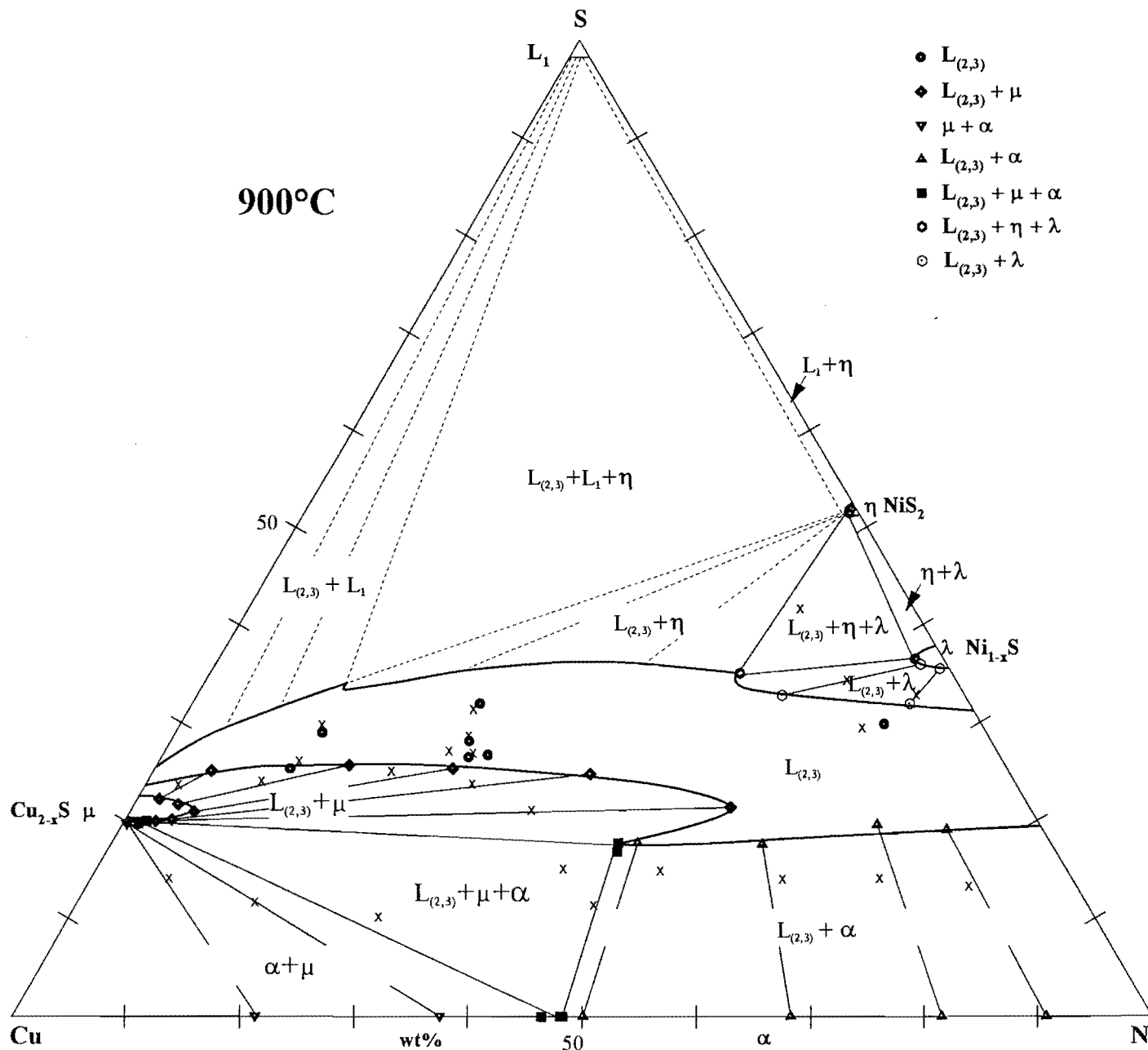


Fig. 2.4: The 900°C isothermal section of the Cu-Ni-S system (Bruwer, 1996).



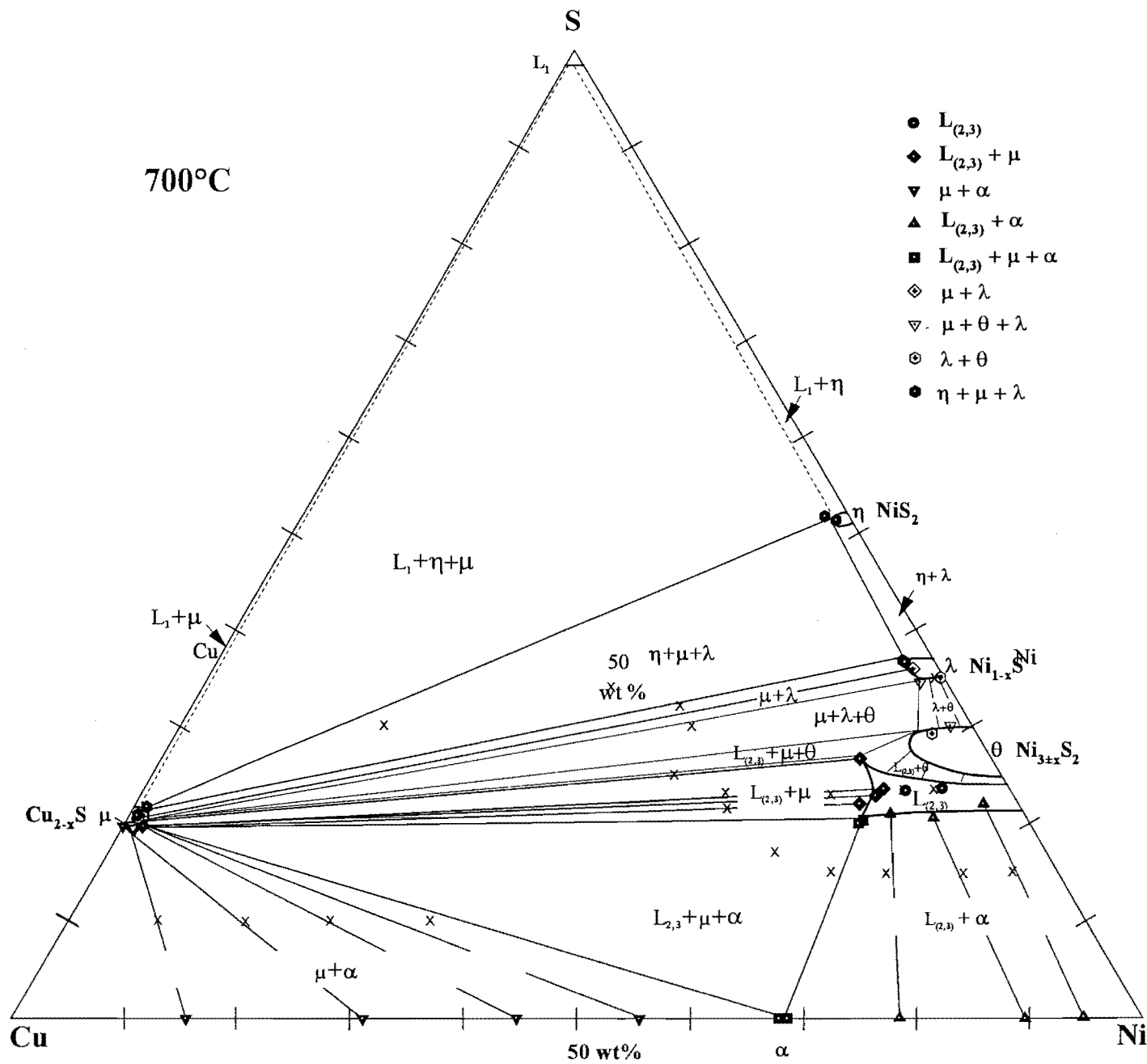


Fig. 2.6: The 700°C isothermal section of the Cu-Ni-S system (Bruwer, 1996).

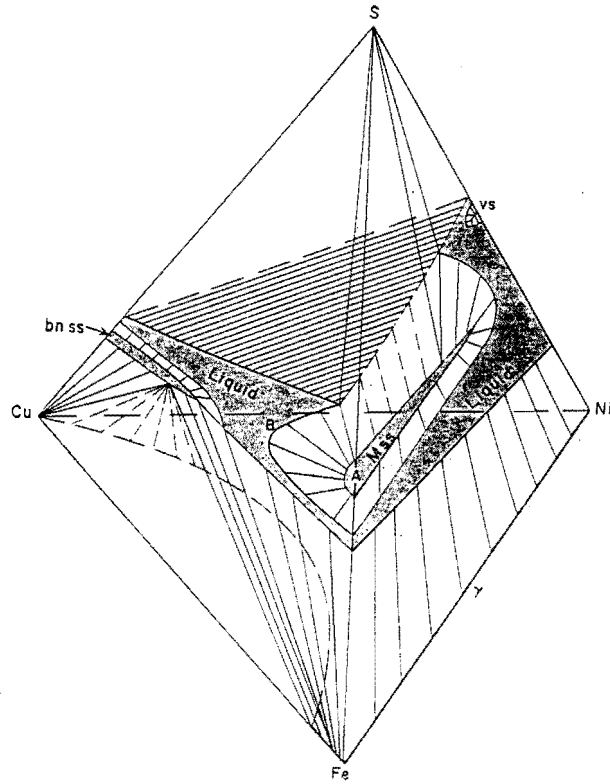


Figure 2.7: Schematic phase relations in the Cu-Ni-Fe-S system at 1000°C (Craig and Kullerud, 1969).

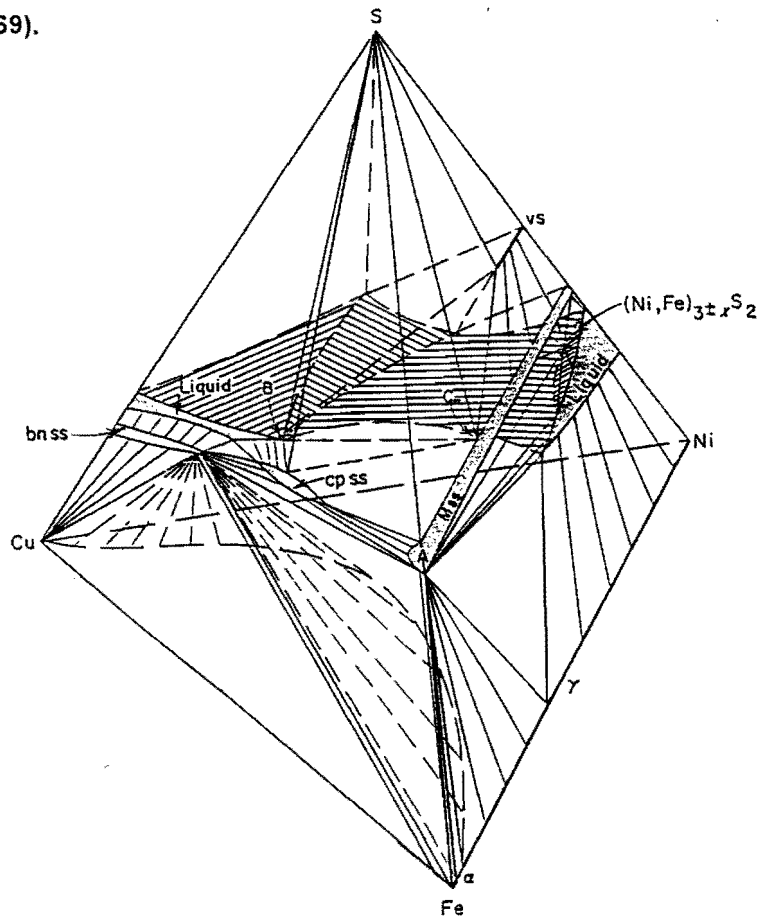


Figure 2.8: Schematic phase relations in the Cu-Ni-Fe-S system at 850°C (Craig and Kullerud, 1969).



### 3. EXPERIMENTAL PROCEDURES

#### 3.1 Planning of Experiments

The phase diagrams of the Cu-Ni-S system (Bruwer, 1996) were used to plan experiments from 700°C to 1200°C in 100°C intervals. Experiments with the same Cu-Ni-S ratios were repeated with only a variation in the Fe content between 1 wt% Fe, 3wt% Fe, 5 wt% Fe and 10 wt% Fe. The total weight of chemicals per experiment was approximate 0.3g.

The first experiments performed were those for the 1000°C isothermal sections with relative short reaction times (1 month), thereafter those for 700°C, which required longer reaction times (2 to 3 months). The experiments at 900°C and 800°C followed with 1100°C and 1200°C completed last (these high temperature experiments required only a few hours reaction time). In retrospect, the reaction times could have been shortened. However, the feeling was to rather extend the reaction time and to ensure equilibrium than to waste consumables. Experiments that clearly failed after reaction were repeated in the next set of preparations.

#### 3.2 Variation in Starting Fe Content

The content of Fe in the experiments was planned as 1, 3, 5 and 10 wt% of the bulk, respectively. However, due to small variations in weighing the powders into the tubes, the proportions of the final product did not always correspond exactly to the planned starting composition. For example, the planned proportions would be: 10 wt% Cu, 65 wt% Ni, 20 wt% S and 5 wt% Fe. After manual weighing all the powdered elements to an accuracy of 4 decimals, the respective weights are: 0.0284g Cu, 0.202g Ni, 0.0582g S and 0.0146g Fe. Recalculation to weight percentage amounts to: 9.37wt% Cu, 66.62 wt% Ni, 19.20 wt% S and 4.82 wt% Fe. This has the effect that a variation in the starting Fe compositions of experiments existed.

#### 3.3 Reduction Techniques

High purity metal powders and powdered sulphur (Table 3.1) were weighed into quartz glass tubes (with an inner diameter of 4mm and an outer diameter of 6mm), evacuated and melt shut at one end. Metal powders had to be reduced first to remove any surface oxidation on the grains. Initially, the metal powders were reduced before the weighing stage in an H<sub>2</sub> - Ar atmosphere, at 600° to 700°C. The system was first flushed with Ar at a temperature of ~ 200° and then the Ar and H<sub>2</sub> gasses were added at an approximate rate of two bubbles per second. After ~ 6 hours the furnace was turned off and the gas shut at the gas bottles – remaining gas in the tubes maintained the closed atmosphere. This method, however, has

some drawbacks: very fine powders have the tendency to fuse together (sinter), making crushing of the powders (which was by hand in an agate crucible) very tedious and long. The concern was that during this long process of crushing and milling, the grain surfaces might undergo oxidation again (especially metallic Fe).

To avoid this problem, a special container was devised to hold the tubes in a horizontal position in a large borosilicate reduction tube within the muffle furnace (Figure 3.1). With this configuration, the gasses were "blown" directly into the small tubes and reacted with the already weighed metal powders. This method was tested in an experiment with a Cu-oxide powder. The Cu-oxide was weighed into two tubes and then placed in the reduction tube at 400°C for ~ 24 hours. The tubes were weighed before and after and an average loss of ~ 10 wt% was measured. The reduced Cu sample was studied in a polished section to determine the degree of reduction. The result was a complete reduction of all the grains right through to the core of each grain.

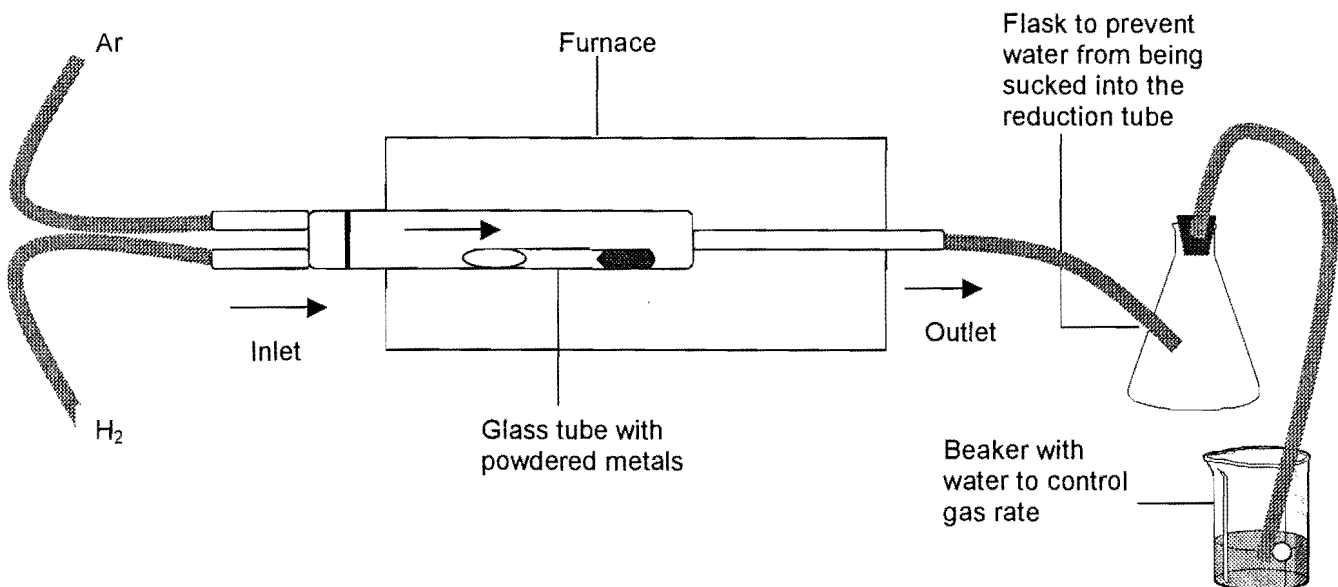


**Figure 3.1 Setup for reduction of metals in quartz glass tubes.**

The metal powders were reduced in the quartz glass tubes at roughly 400°C (the softening temperature for borosilicate is 820°C) for approximate 12 hours. Immediately after reduction of the metals, dried sulphur powder was added. The powders were covered with a tight fitting quartz glass rod and then the tube was sealed off under vacuum ( $\sim 2 \times 10^{-2}$  millibar). After each sample was weighed (and sometimes the length recorded to distinguish between samples), the samples were ready to be pre-reacted.

**Table 3.1: The percentage purity of chemicals used in experiments of the Cu-Ni-Fe-S system.**

| Chemical    | Purity   |
|-------------|----------|
| Copper (Cu) | 99.999 % |
| Nickel (Ni) | 99.99+%  |
| Iron (Fe)   | 99.99    |
| Sulphur (S) | 99.99+   |

### 3.4 Heating Techniques

Samples were first placed into a pre-reaction furnace at a temperature between 500° and 700°C. This step was included to ensure that all the free sulphur reacted with the metals. At sudden high temperatures, solid sulphur would turn to gas and result in violent explosions because the sealed glass tube can not withstand such a rapid increase in volume. Limited reaction (of which the extend is difficult to measure without opening the tube) will occur between metals depending on the duration of pre-reaction. After sufficient reaction took place (i.e. not free sulphur visible) samples were quenched in air or immediately transferred to the reaction furnace. To prevent unnecessary strain on the glass, it was found to be better not to quench the samples after pre-reaction, but to proceed immediately to the required reaction temperature.

Samples were then placed into a high-temperature furnace with an accuracy of 1°C (verified with an external thermocouple). The furnaces used for equilibrium reactions were modified to hold 6 corundum tubes with an inner diameter of about 45mm. This modification allows six positions into which samples could be placed. If one sample would brake in one tube the samples in the other tubes were not affected. It was also possible to determine the hot zone in each tube, and to position samples exactly there. However, not all of the six corundum tubes' hot zone were equal in temperature. There was a difference in temperature between tubes of up to 25°C at lower temperatures. This was overcome by measuring the temperature with an external K-type thermocouple and increasing the temperature until the "coolest" tube was at the required temperature in its hot-zone. The thermocouple was again used to determine that position in the other tubes where the desired temperature prevailed.

Initially the samples were melted at a high temperature (between 1000° and 1100°C) to achieve homogenization throughout the entire sample. After a couple of hours the temperature was lowered to the required equilibrium temperature. This melting stage was later abandoned because of early and frequent breakages of the quartz glass tubes. Longer pre-reaction times were found to be sufficient to ensure equilibrium reactions.

The time required to achieve equilibration depends on the temperature and type of reactions investigated. At high temperatures (e.g. >1000°C), reactions take place fast, but at lower

temperatures (e.g.  $< 800^{\circ}\text{C}$ ), reactions may be hampered by slow reaction kinetics (e.g. the gradual change from a mono-sulphide to a di-sulphide as in the case with Ni-S to  $\text{NiS}_2$ ). Therefore, the time required to achieve equilibrium could take anything from 2 weeks to 2 months or more.

After equilibrium was completed the samples were quenched in water by dropping it in a long cylindrical container. The temperature in the sample dropped within seconds from hundreds of degrees to room temperature. Samples were weighed again to identify each one and then the contents were described. In some experiments, the reactants separated and the extent of equilibrium was uncertain. Physical separation of solids from the melt due to density differences might cause separation, or surface tension between two melts could have caused them to detach from each other. Separation might also be a result of movement during quenching and does not always imply separation during reaction and dis-equilibrium. Experiments that contained two or more separate pieces after quenching were usually discarded and repeated.

### 3.5 Mounting and Labeling Technique

The glass tubes were carefully broken to release the contents in one piece. The reacted sample was then divided (with a stainless steel knife and a small hammer) into two pieces: one piece was used in a polished section and the other piece was stored as a reference. Because of the size of the samples ( $< 4\text{mm}$ ), an average of 5 samples were mounted in one section (with a diameter of  $2.5\text{cm}$ ) (Figure 3.2) together with a reference Cu-rod. The sections were labeled using the equilibration temperature and an alphabetic symbol. The experiment number carried the section label followed by a number (1 to 5) indicating the position on the section (after polishing) in a clockwise direction.

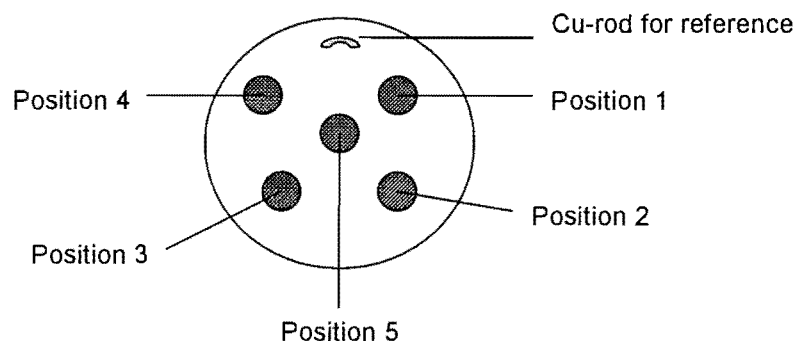


**Figure 3.2: Example of a polished section; indicated are the position of the reference Cu-rod and the other positions on the sample.**

i 16031738  
b1543123x

### 3.5 Descriptive Techniques

Sections were polished and then described using a reflected light microscope. Sections were carefully studied for the presence of small oxide phases that indicated that the experiment was not conducted in a closed four-element system. The glass tube might have cracked during reaction and allowed air to penetrate the sample. Photographs taken of each experiment at different magnifications assisted in the analytical procedures and served as visual reference.

### 3.6 Experimental Difficulties

A large number of experiments failed due to cracking of the quartz glass tube during either pre-reaction or reaction. It is believed the particular batch of quartz glass available for these experiments, was not of a suitable quality to withstand reaction at high temperatures (typically higher than 1000°C) or quenching from high temperatures. Eliminating the melting stage and limiting equilibrium reactions at temperatures above 1000°C to a few hours, did help to prevent cracking of the glass. All future experiments were conducted in this fashion to prevent a repetition of such an event with other quartz glass batches.

In some experiments the tapered tip of the glass tube resulting from melting the tube shut at one end caused zoning or uneven mixing of the reactants during reaction. An attempt to limit zoning or separation was made by altering the arrangement of reactants in the tube: A glass rod was placed into the tube first, then the metal- and sulphur powders and then another piece of rod. The tube was then sealed off under vacuum (Figure 3.3). After reaction and quenching of four test samples, the metal-sulphur sample in all of the experiments were in one piece with no external indications of zonation or separation.

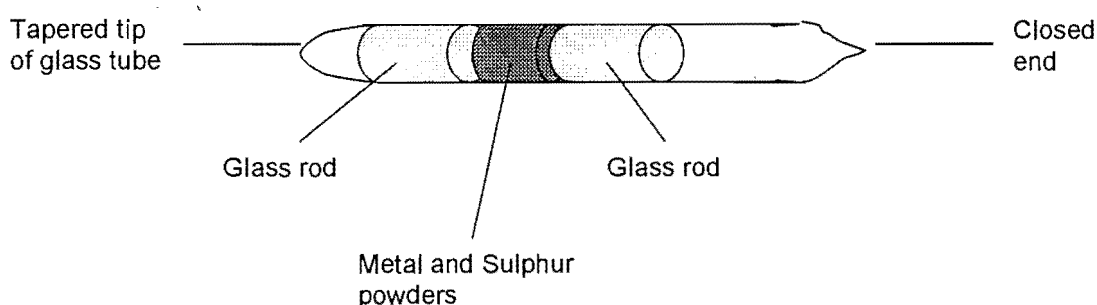


**Figure 3.3:** The configuration for some of the experimental samples. A quartz glass rod is placed at both ends of the metal and sulphur powders, and then the quartz glass tube is sealed under vacuum.

The second problem of separation of material in the tube during equilibration, is mainly attributed to the fact that a larger volume is left in the tube after reaction of the sulphur with the metals. After quenching it could not be determined whether separation took place during

reaction or during quenching. In the first instance the experiment would be in dis-equilibrium but this is not the case in the second instance. The separated pieces could be re-tubed, but this required grinding and milling of the material to reduce the occupied space in the quartz tube. The process of grinding and milling an already reacted sample was very time consuming and mostly not practical due to the toughness of the alloy in particular. Some of the original starting material was lost in this procedure, and the possibility of oxidation during milling (especially if Fe is present) was an unmeasurable factor to take into account. Normally, a sample of each separated piece was mounted and evaluated optically and analytically to determine dis-equilibrium, based on compositional variation exceeding an analytical uncertainty at the  $1 \sigma$  level. If dis-equilibrium was suspected the entire experiment was repeated with newly weighed material.

## 4. ANALYTICAL PROCEDURES

### 4.1 Analytical Preparation

The polished sections were cleaned and coated with a thin carbon layer (~200 nm) to ensure good conductivity, then placed in a desecrator to keep it dry and free of contamination until it could be analyzed.

### 4.2 Analytical Techniques

A JEOL Superprobe 733 were used for the wavelength dispersive analyses at a beam current of 20nA and an acceleration potential of 20kv. For large homogeneous phases (i.e. alloys and sulphides) spot analyses were used, and for heterogeneous phases (i.e. sulphides with exsolutions or quenched melts) a defocused beam (with diameter of 40 $\mu$ m) or area analyses (of 1.5 $\mu$ m x 2.0 $\mu$ m) were most effective. Pure Cu, Ni and Fe metals were used as standards for the alloy phases, and millerite, chalcopyrite and troilite were mostly used as standard for the sulphide and melt phases.

A peak seek was performed daily on all the elements to be measured for a specific phase. A general standardization or re-calibration followed, during which the counts for each element (background as well as at peak positions) were detected and compared with the previous day's counts. Counting time on the background was 25 seconds and on the peak 50 seconds. A change in count rates due to some mechanical problem could easily be detected and steps taken to improve conditions for measurement.

Difficulties encountered in collecting electron microprobe (EMP) analyses of quenched sulphide melts are the generally coarse grained texture of these melts and the lack of suitable standards. A sulphide melt cannot be quenched like a silicate melt, but crystallizes in a fine intergrowth of different phases. If spot analyses are used, a large number of single analyses on a closely spaced grid must be collected to obtain a representative composition of the melt in total. The availability of analytical time will influence the number of analyses that can be collected from a single melt phase. In area analyses, the beam is scanning a selected area and only remains on one position for a very short period of time during which data is collected. After the required counting time, the analytical result is representative of the composition of the area. This method requires (apart from a standard with the same phases and textures, see below) that a large enough area (consisting only of melt) is available for analysis. In this investigation, suitable areas for area-analysis could not always be defined. The method of defocused beam analysis involves increasing the diameter of the beam spot to a size larger than most of the grain sizes in the quenched melt. The composition of a small round area is then given, and the mean value of a number of small areas is taken as the average composition. In experiments, where only a small portion of the quenched melt is

intersected in the polished section, this method worked best. However, in situations like these, the possibility of collecting data that fully represent the melt becomes very limited.

In an attempt to improve the results of coarse textured quenched melt phases, melt standards with a known chemical composition were produced in the lab and quenched from 1200°C. These standards differ in composition and texture. Although the standards did not always match exactly the texture and composition of the unknown melt phase, analytical results are in most cases considered “good” (i.e. small standard deviations and matching tie-line angles).

The area and number of analyses were selected based on the texture of the phase to be analyzed. Therefore, an overview on the textural appearance of the different phases is given in the next chapter.

#### 4.3 Reproducibility Tests

To determine the reproducibility of the data, duplicate analyses were collected under identical conditions from alloys and exsolution-free sulphides (Table 4.1). Analyzed twice, the same analytical point should under identical conditions result in identical composition. However, due to variations in the mechanical and electronic conditions as well as normal variations in counting statistics, the values are not identical for each element analyzed. By determining the deviation from duplicate analyses, these variations become quantifiable. The deviation of analytical results given in the EMP analyses could be determined. Any larger variation in the composition will be due to true compositional variations.

The standard deviation was derived, following the recommendations of Kaiser and Specker (1956), with the formula:

$$s = \sqrt{\frac{\sum_1^{N/2} (v_i - v_j)^2}{N}}$$

Where: s = standard deviation (1s)

v = duplicate analyses

N = number of analyses



Table 4.1: Reproducibility results for alloy, digenite, millerite and vaesite.

| Alloy 1  |               |           |           | Alloy 2  |               |           |           | Alloy 3  |               |           |           |
|----------|---------------|-----------|-----------|----------|---------------|-----------|-----------|----------|---------------|-----------|-----------|
| Elements | Range         | Std. Dev. | No. Anal. | Elements | Range         | Std. Dev. | No. Anal. | Elements | Range         | Std. Dev. | No. Anal. |
| Cu       | 44.47 - 42.32 | 0.42      | 20        | Cu       | 42.66 - 40.22 | 0.50      | 20        | Cu       | 45.04 - 40.02 | 0.37      | 20        |
| Ni       | 53.81 - 50.19 | 0.21      | 20        | Ni       | 52.87 - 51.35 | 0.17      | 20        | Ni       | 50.63 - 48.03 | 0.19      | 20        |
| Fe       | 1.29 - 1.20   | 0.01      | 20        | Fe       | 2.64 - 2.54   | 0.03      | 20        | Fe       | 5.50 - 4.56   | 0.02      | 20        |

| Digenite 1 |               |           |           | Digenite 2 |               |           |           | Digenite 3 |               |           |           |
|------------|---------------|-----------|-----------|------------|---------------|-----------|-----------|------------|---------------|-----------|-----------|
| Elements   | Range         | Std. Dev. | No. Anal. | Elements   | Range         | Std. Dev. | No. Anal. | Elements   | Range         | Std. Dev. | No. Anal. |
| Cu         | 74.27 - 69.94 | 0.48      | 30        | Cu         | 77.24 - 73.45 | 0.64      | 28        | Cu         | 74.66 - 70.22 | 0.59      | 28        |
| Ni         | 0.87 - 0.12   | 0.03      | 30        | Ni         | 1.45 - .24    | 0.01      | 28        | Ni         | 0.31 - 0.07   | 0.01      | 28        |
| Fe         | 2.05 - 1.81   | 0.03      | 30        | Fe         | 0.36 - 0.09   | 0.03      | 28        | Fe         | 1.38 - 0.30   | 0.12      | 28        |
| S          | 21.71 - 21.04 | 0.14      | 30        | S          | 19.80 - 18.99 | 0.12      | 28        | S          | 20.09 - 19.09 | 0.14      | 28        |

| Millerite 1 |               |           |           | Millerite 2 |               |           |           | Millerite 3 |               |           |           |
|-------------|---------------|-----------|-----------|-------------|---------------|-----------|-----------|-------------|---------------|-----------|-----------|
| Elements    | Range         | Std. Dev. | No. Anal. | Elements    | Range         | Std. Dev. | No. Anal. | Elements    | Range         | Std. Dev. | No. Anal. |
| Cu          | 2.50 - 0.52   | 0.09      | 30        | Cu          | 0.12 - 0.06   | 0.02      | 30        | Cu          | 3.15 - 0.68   | 0.05      | 30        |
| Ni          | 61.07 - 57.73 | 0.38      | 30        | Ni          | 61.41 - 59.27 | 0.54      | 30        | Ni          | 59.12 - 56.16 | 0.35      | 30        |
| Fe          | 0.82 - 0.75   | 0.01      | 30        | Fe          | 1.26 - 1.18   | 0.02      | 30        | Fe          | 1.69 - 1.52   | 0.02      | 30        |
| S           | 39.42 - 36.04 | 0.15      | 30        | S           | 37.53 - 36.69 | 0.20      | 30        | S           | 37.46 - 36.40 | 0.22      | 30        |

| Vaesite 1 |               |           |           | Vaesite 2 |               |           |           | Vaesite 3 |               |           |           |
|-----------|---------------|-----------|-----------|-----------|---------------|-----------|-----------|-----------|---------------|-----------|-----------|
| Elements  | Range         | Std. Dev. | No. Anal. | Elements  | Range         | Std. Dev. | No. Anal. | Elements  | Range         | Std. Dev. | No. Anal. |
| Cu        | 1.80 - 1.03   | 0.06      | 28        | Cu        | 0.10 - 0.05   | 0.01      | 30        | Cu        | 3.52 - 0.51   | 0.03      | 56        |
| Ni        | 46.95 - 45.28 | 0.40      | 28        | Ni        | 47.90 - 45.80 | 0.24      | 30        | Ni        | 46.84 - 43.02 | 0.39      | 56        |
| Fe        | 0.16 - 0.06   | 0.01      | 28        | Fe        | 0.49 - 0.12   | 0.01      | 30        | Fe        | 0.23 - 0.04   | 0.01      | 56        |
| S         | 52.21 - 49.73 | 0.26      | 28        | S         | 52.33 - 50.72 | 0.19      | 30        | S         | 52.20 - 51.36 | 0.26      | 56        |

#### 4.4 Data Evaluation

At the start of the project, a large number of analyses were collected of seemingly homogeneous phases to ensure that there is no change in composition from the rim to the center of the mineral phase. After homogeneity was confirmed of alloys and exsolution-free sulphide phases, the amount of analyses were decreased considerably.

Precision is determined by the reproducibility of analytical results, while accuracy is displayed in the resemblance of analyzed results to expected results. High precision was achieved by frequent standardization and control measurements on standards, as well as monitoring the count rates on these standards. A high kV and mA, and a stable electron beam increased the total counts and decrease the statistical variation that was determined by the number of counts. High accuracy was obtained by testing the standardization on a specimen with known composition and correcting any deviations larger than  $\pm 3s$  that is not due to the heterogeneity of the specimen.

Data were carefully evaluated and the reliability of analyses were tested statistically. Because most of the quenched melts are heterogeneous with two or three components, the standard deviations of the melt analyses are relatively high in comparison with the alloy and sulphide phases. It was therefore felt necessary to follow an independent approach to determine the average composition of the melt and the reliability of this average value. This was conducted by applying Resampling Statistics (Simon, 1997; Westfall & Young, 1992) which involves the random selection of analyses from a data set. The selection is repeated for e.g. 15000 times, each time using the original data set as a "pool" to construct a new data set. The original data set is thus randomly duplicated to create a new data set with much more data. Statistical calculations of this new data set will be a closer representation of the smaller data set. An example of such a recalculation is given in Appendix A.

After resampling was performed on the analyses from selected melt phases, the mean values did not change (which underlines the reliability of the analytical approach) but the confidence intervals (ci) for the average composition of these melts were much better defined. EMP results treated in this manner are indicated on the tables for the different equilibrium temperatures (Appendix C). The total number of successful experiments carried out and electron microprobe analyses collected are summarized in Table 4.2.

**Table 4.2: Total amount of experiments and analyses.**

| Temperature  | Total Experiments | Total Analyses |
|--------------|-------------------|----------------|
| 1200         | 22                | 1348           |
| 1100         | 31                | 2947           |
| 1000         | 41                | 3141           |
| 900          | 60                | 5589           |
| 800          | 61                | 4632           |
| 700          | 36                | 2905           |
| <b>Total</b> | <b>251</b>        | <b>20562</b>   |

The means of the recalculated values were plotted on quaternary and ternary diagrams with the aid of a statistics package (Statistica). Due to limitations in displaying a four component system in two

dimensions it was necessary to evaluate the shape of the liquidus in the third dimension, and whether a projection onto the Cu-Ni-S ternary is an acceptable estimation.

In a system with three components at a fixed temperature and pressure, an univariant point (i.e. a position in a two phase field like Alloy+Melt) will have one degree of freedom according to the phase rule.

$$P + F = C + 2$$

(where P = number of phases, F = degrees of freedom, C = number of components)

$$2 + F = 3 + 0$$

$$F = 1$$

However, in a four component system, the degrees of freedom is two:

$$P + F = C + 2$$

$$2 + F = 4$$

$$F = 2$$

This implies that to uniquely define a tie-line in this two-phase field, two variables must be fixed. If the Cu/Ni ratio in the starting composition and the temperature of equilibration is fixed, a plot of the Fe: S content in the melt will give an indication of the shape of the liquidus in the dimension not observed in the projection onto the Cu-Ni-S ternary. This was evaluated for 4 experiments at 1200°C and 4 experiments at 1100°C temperature intervals (Table 4.3 and Fig. 4.1). These experiments have the same Cu/Ni ratio i.e. ~ 0.12 at 1200°C and ~ 0.50 at 1100°C. Incorporating the 95% confidence intervals, the sulphur content in the melt could not be safely distinguished (the lower sulphur content of experiment 12m4 is attributed to a small proportion of a very coarse grained melt which contains large dendritic alloy). This plot shows that although the shape of the liquidus in the third dimension for small quantities of Fe is not smooth, the slope is still very steep and that a projection from a prism onto the Cu-Ni-S ternary will be valid for descriptive purposes. Projections from a prism appear similar to plots in a Fe-free system as shown in Figures 4.2 and 4.3. A numerical example of the conversion of a bulk composition to the plotted values in the Cu-Ni-S ternary, is given in Table 4.4.

**Table 4.3: The EMP results for the melt phase in the assemblage (Alloy+Melt) from experiments at 1200°C and 1100°C and a Cu/Ni ratio in the starting composition of ~ 0.12 and ~ 0.50 respectively (ci = 95% confidence interval).**

| <b>1200°C</b> | <b>Exp. No.</b> | <b>Fe</b> | <b>S</b> | <b>ci for S</b> | <b>S - ci</b> | <b>S + ci</b> |
|---------------|-----------------|-----------|----------|-----------------|---------------|---------------|
|               | 12l4            | 0.52      | 19.21    | 1.41            | 17.80         | 20.62         |
|               | 12m4            | 1.09      | 16.16    | 1.41            | 14.75         | 17.57         |
|               | 12n4            | 1.42      | 20.37    | 1.33            | 19.04         | 21.70         |
|               | 12o4            | 4.03      | 20.04    | 0.93            | 19.11         | 20.97         |
| <b>1100°C</b> | <b>Exp. No.</b> | <b>Fe</b> | <b>S</b> | <b>ci for S</b> | <b>S - ci</b> | <b>S + ci</b> |
|               | 11b3            | 0.52      | 15.95    | 1.21            | 14.74         | 17.16         |
|               | 11d3            | 2.20      | 13.82    | 1.34            | 12.48         | 15.16         |
|               | 11f2            | 3.00      | 14.47    | 1.20            | 13.27         | 15.67         |
|               | 11h3            | 6.19      | 15.21    | 0.97            | 14.24         | 16.18         |

**Table 4.4: A numerical example of the conversion of a bulk composition to the plotted Cu, Ni, S values. For a projection onto the ternary Cu-Ni-S plane, the value of Fe is taken to be 0.**

| Bulk composition |       |      |      |       | Normalized values |                 |    |                |       |
|------------------|-------|------|------|-------|-------------------|-----------------|----|----------------|-------|
| Cu               | Ni    | Fe   | S    | Total | Cu                | Ni              | Fe | S              | Total |
| 27.33            | 54.55 | 8.94 | 9.18 | 100   | 27.33/<br>91.06   | 54.55/<br>91.06 | 0  | 9.18/<br>91.06 | 1     |
| 27.33            | 54.55 | 0    | 9.18 | 91.06 | X100              | X100            |    | X100           | X100  |
|                  |       |      |      |       | 30.01             | 59.91           | 0  | 10.08          | 100   |

If the starting composition indicates that the experiment did fall into a multi-phase stability field but not all of the phases in the assemblage occur in the section, it was assumed that other phases could exist. It was decided not to grind the polished section down any further for fear of losing other experiments in the same section (that have a different three-dimensional size). For example, in the 3 component stability field containing the cotectic alloy, digenite and melt (Fig. 4.4), some of these phases may not be intersected in the polished section. If the starting composition and/or the composition of the observed phases indicate that the experiment does fall into this field then the observed phase(s) were treated as being part of a 3-phase assemblage. In cases where more than one experiment (in the same isothermal section) forms part of the same 3-phase assemblage the mean values of the phases from the different experiments were calculated.

Starting compositions are not indicated on the phase diagrams to simplify the diagrams, but are given in Appendix B. Dotted tie-lines are extrapolation to a composition based on the direction of adjacent tie-lines and/or available field boundary lines. Dotted field boundary lines are indications of where the stability fields could be, but are not well defined due to insufficient data points.

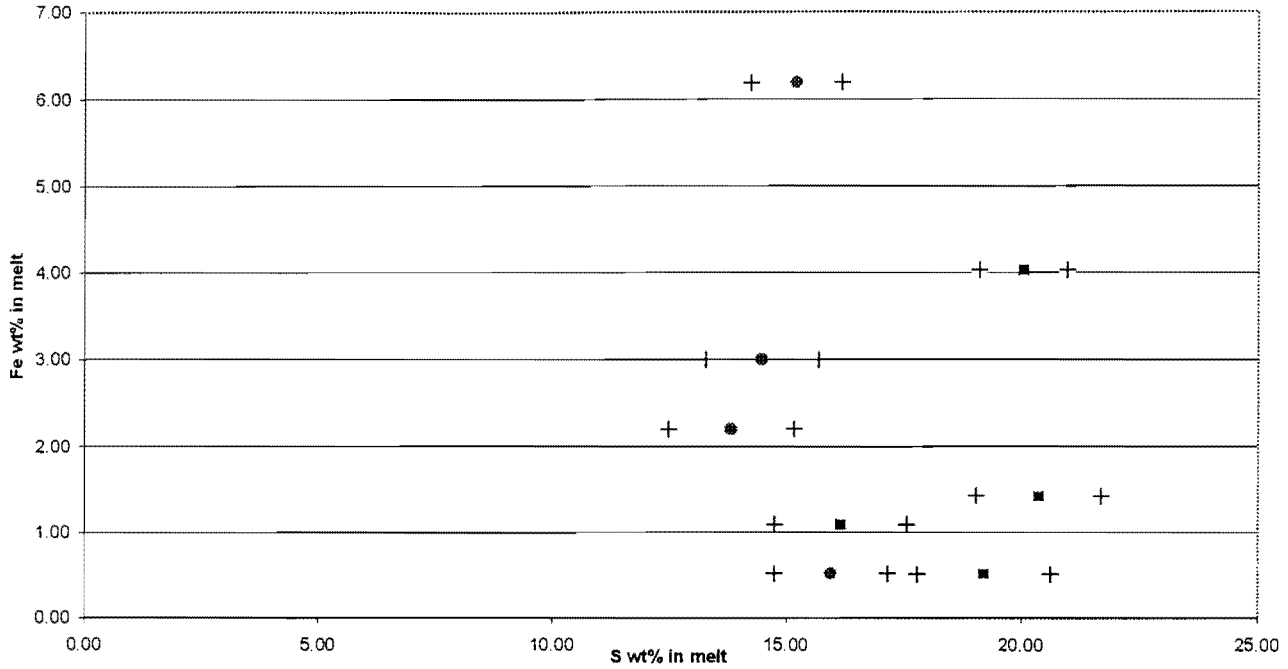


Figure 4.1 :Composition of melt in equilibrium with alloy. At 1200°C (squares) with a Cu/Ni of  $-0.12$  and at 1100°C (circles) with a Cu/Ni ratio of  $-0.50$ . Also indicated are the 95% confidence intervals (crosses).

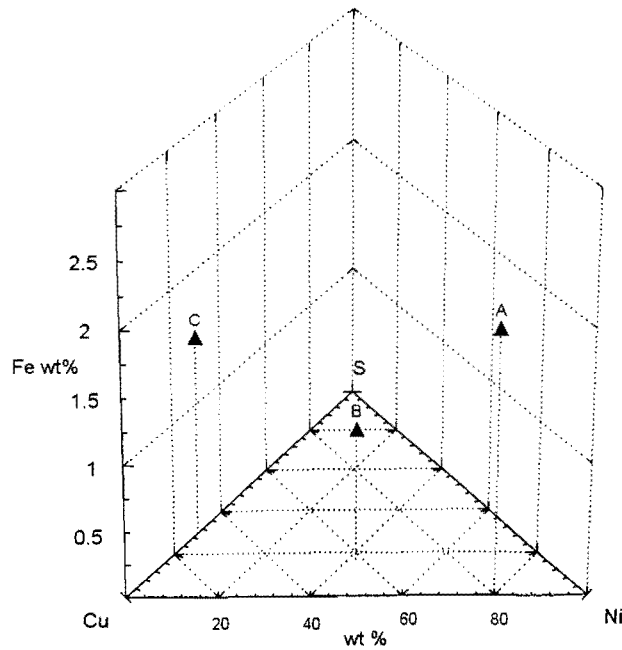


Figure 4.2: A graphic presentation of three data points (A, B and C) in a quaternary diagram. The axis for Fe extends perpendicular to the triangle into the third dimension

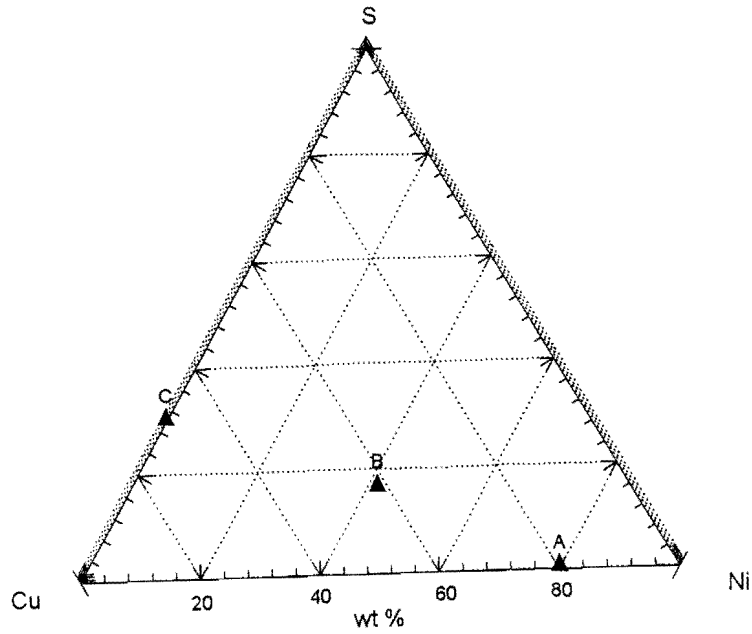


Figure 4.3: A projection of the three data points (A, B and C) onto the floor of the quaternary diagram. This plot is similar to a plot in the Fe-free ternary system Cu-Ni-S, and the Fe value of the points can not be derived from this plot.

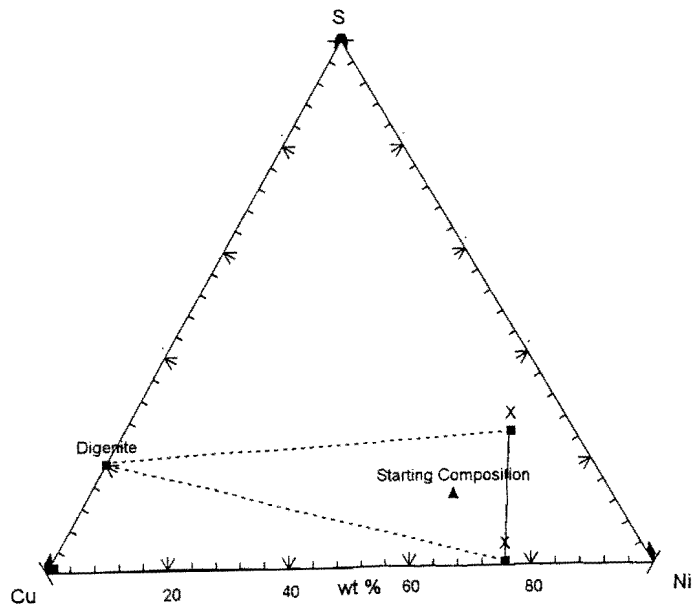


Figure 4.4: The starting composition indicates that the experiment x falls into the three component stability field, even though only two of the three phases (marked x) are observed.

Obtaining a representative section is also influenced by the phases present. If a large amount of alloy is present, brittle sulphides and quenched melts are likely to break in small pieces and detach from the harder alloys during cutting. Experiments containing only alloy and digenite often formed a spongy texture. During grinding and polishing of such a sample, the brittle digenite might be ripped out from between the alloy in the sample.

The solid phases are texturally and compositionally homogeneous, with the exception of exsolution textures in digenite and some millerite. Sulphide melts can not be quenched successfully and therefore represent mixtures of crystallized sulphide and/or alloys, giving it a heterogeneous texture.

### 5.1 Alloys

Alloy phases occur mostly as well defined homogeneous grains. There are no compositional or textural differences between the core and the rims of the alloy grains. The rims of the grains are mostly smooth but sometimes appear uneven with evaginations when in contact with a melt in which alloy is one of the components (Photograph 5.1). It appears that small alloy grains, which formed on quenching from the melt, overgrow onto the larger (older) alloy grain. The small alloy grains in a quenched melt phase often appear as perfectly euhedral crystals (Photograph 5.2) which may arrange themselves in skeletal patterns (Photograph 5.3).

### 5.2 Digenite

Digenite has a light blue colour in plane polarized light and occurs as irregular or rounded grains. In quenched melt, digenite often displays skeletal growth patterns (Photograph 5.4). Digenite may, or may not, contain exsolutions, depending on the equilibrium temperature.

Exsolution-free digenite occurs in association with an alloy phase at temperatures lower than 900°C. Frequently, these exsolution-free digenite contains blobs of metallic Cu at the contacts with the alloy or around gas bubbles in the digenite (Photograph 5.5). The appearance of metallic Cu is not exclusive to exsolution-free digenite but also occurs in assemblages of digenite with exsolutions. A rim of metallic Cu at the contact of exsolution-digenite with melt was occasionally observed.

In digenite with exsolutions, two types of exsolutions occur: skeletal exsolutions (Photograph 5.6) and round exsolutions (Photograph 5.7). The round exsolutions are far more common and vary in size and abundance. Both types of exsolutions can appear together in digenite. In most of the experiments, the exsolutions (both round and skeletal exsolutions) will disappear towards the contact of the digenite grain with other phases. In some experiments, a thin exsolution rim of a Ni-rich sulphide phase was observed at the contact between the digenite and the adjacent phase.

### 5.3 $\beta$ -phase

At 800°C and lower, a phase was observed that is optically and chemically different from digenite. In plane polarized reflected light this phase appears brownish and tarnishes easily (it also has a completely different color than digenite when coated with carbon). It is not stoichiometric bornite but contains more sulphur and less Cu than digenite and will be referred to as phase " $\beta$ ".  $\beta$ -phase was only observed in assemblages with vaesite, millerite and melt (i.e. with starting compositions high in sulphur). It always contained round exsolutions of the same type that was observed in digenite (Photograph 5.8). Digenite and  $\beta$ -phase were never observed in the same experiment. This phase will be discussed more comprehensively in chapter 7.

### 5.4 Covellite

Covellite only occurred in very small quantities adjacent to digenite or  $\beta$ -phase (Photograph 5.9). Kullerud (1965) investigated the stability relations of covellite in the Cu-S system and found that covellite breaks down to digenite and sulphur above 507°C. The presence of covellite in some experiments may indicate a metastable existence due to fast quenching.

### 5.5 Millerite

Millerite appears yellow and slightly pleochroic in normal polarized light. The millerite grains are anhedral and may contain round (Photograph 5.10) or flame-like exsolutions (Photograph 5.11) of a Cu-rich sulphide. These exsolutions are too small to quantify the exact composition.

### 5.6 Vaesite

Vaesite has a gray color in plane polarized light, and appears as subhedral or anhedral grains. No exsolutions were observed, but uneven round "inclusions", that appear like gas bubbles, were occasionally detected in the center of grains (Photograph 5.12).

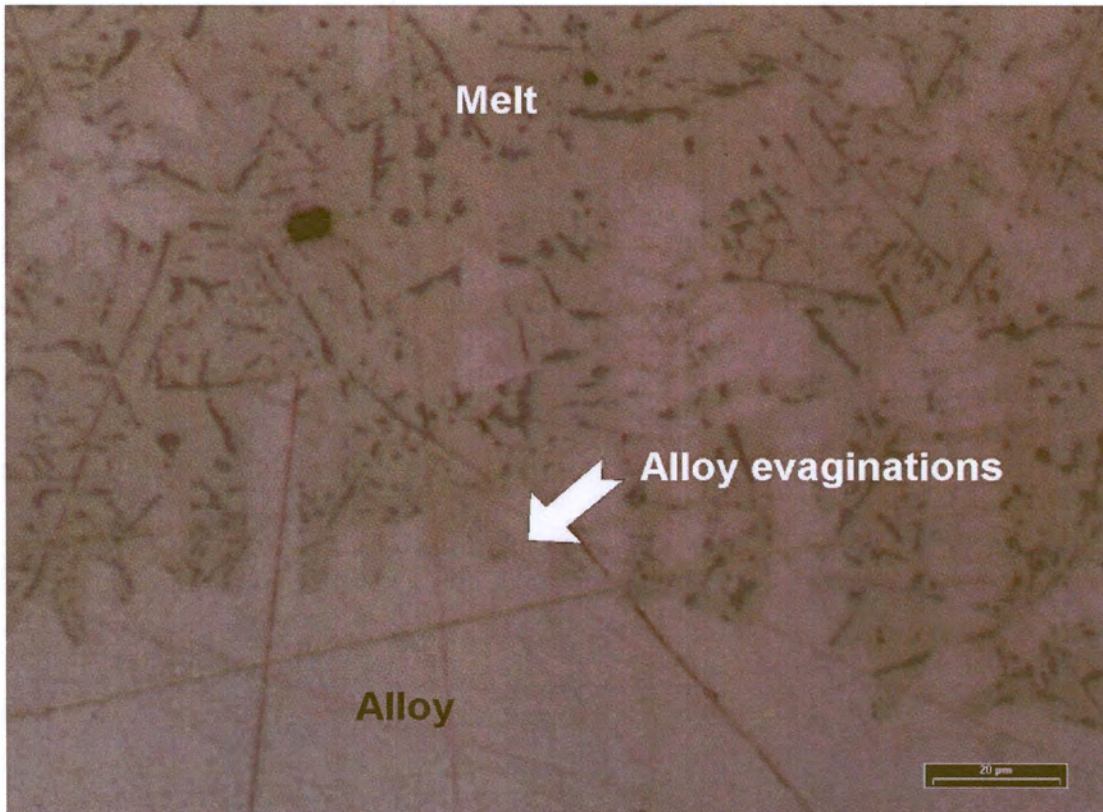
### 5.7 Melt

The term "melt" refers to the component of the experiment that was still liquid at the time of quenching, but that had cooled down relatively quickly to produce a mixture of phases. The aim when quenching was to produce the finest texture possible, but textures depend on the cooling rate, the starting composition (i.e. proportion and type of solids to melts) and the crystallization temperatures of phases that form on quenching. Diffusion speeds are higher at higher temperatures, so if the composition causes a phase to start crystallizing at higher temperature, it will be coarser. The degree of heterogeneity (i.e. variations in sites of crystallites) differs from experiment to experiment.

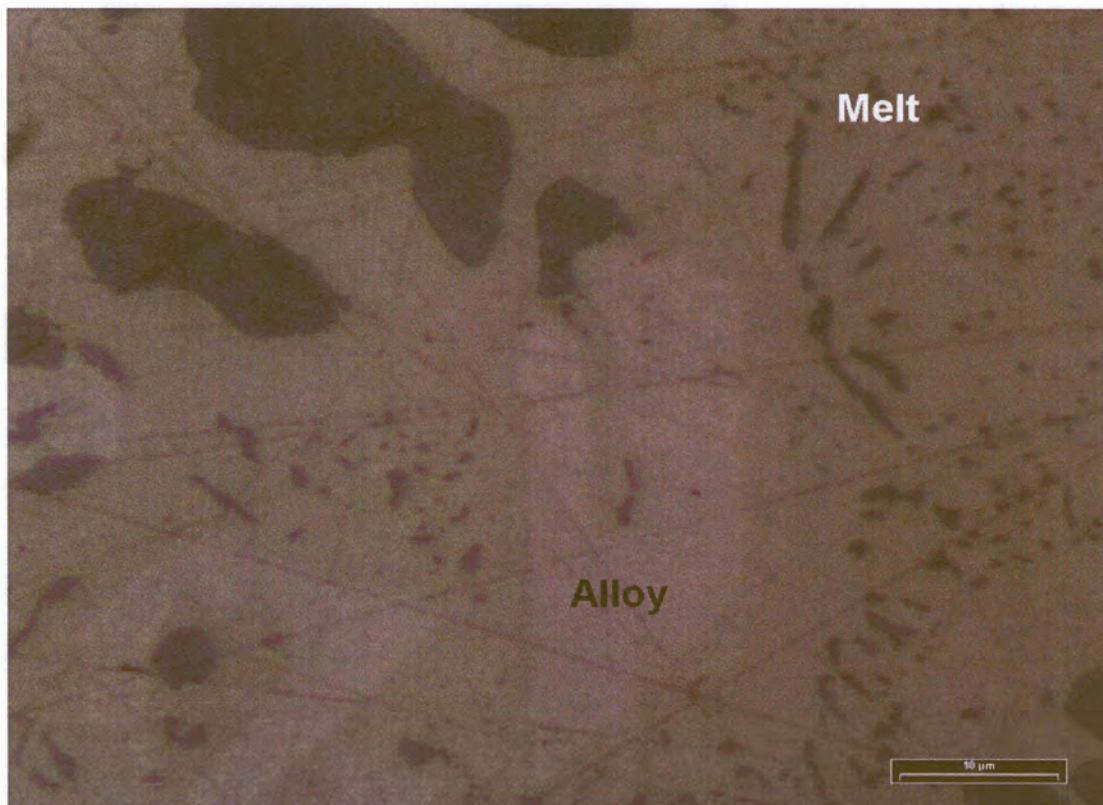
Melts in the (alloy+digenite+melt)-assemblage consist of euhedral or skeletal alloy grains, dendritic digenite and a groundmass of a Ni-sulphide (Photograph 5.13). In the melt with a Cu-rich starting composition, the proportion of digenite to Ni-sulphide is high (Photograph 5.14), and likewise the melt



from a Ni-rich starting composition has a higher proportion of Ni-sulphide than digenite (Photograph 5.15). The proportion of alloy in such melts is fairly constant but the composition of the alloy is variable. The melts co-existing only with sulphide(s) have no alloy component (Photograph 5.16).



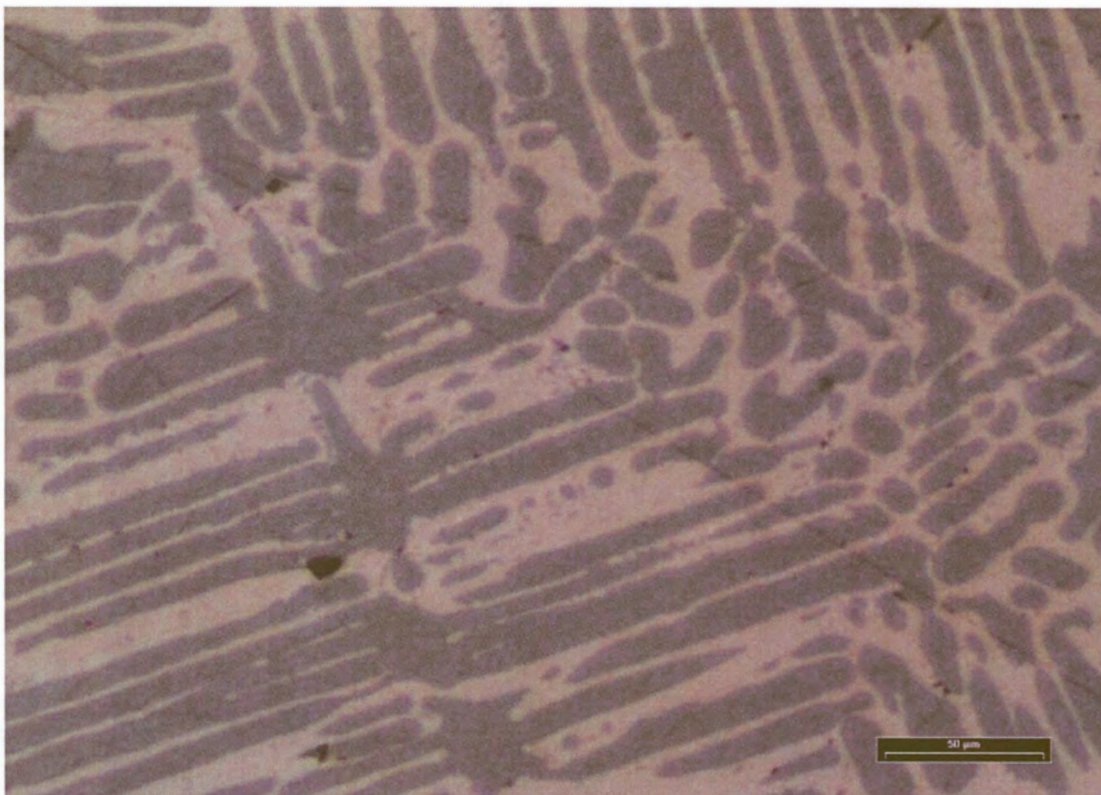
Photograph 5.1: Alloy and associated melt with evaginations of alloy (experiment 7d2).



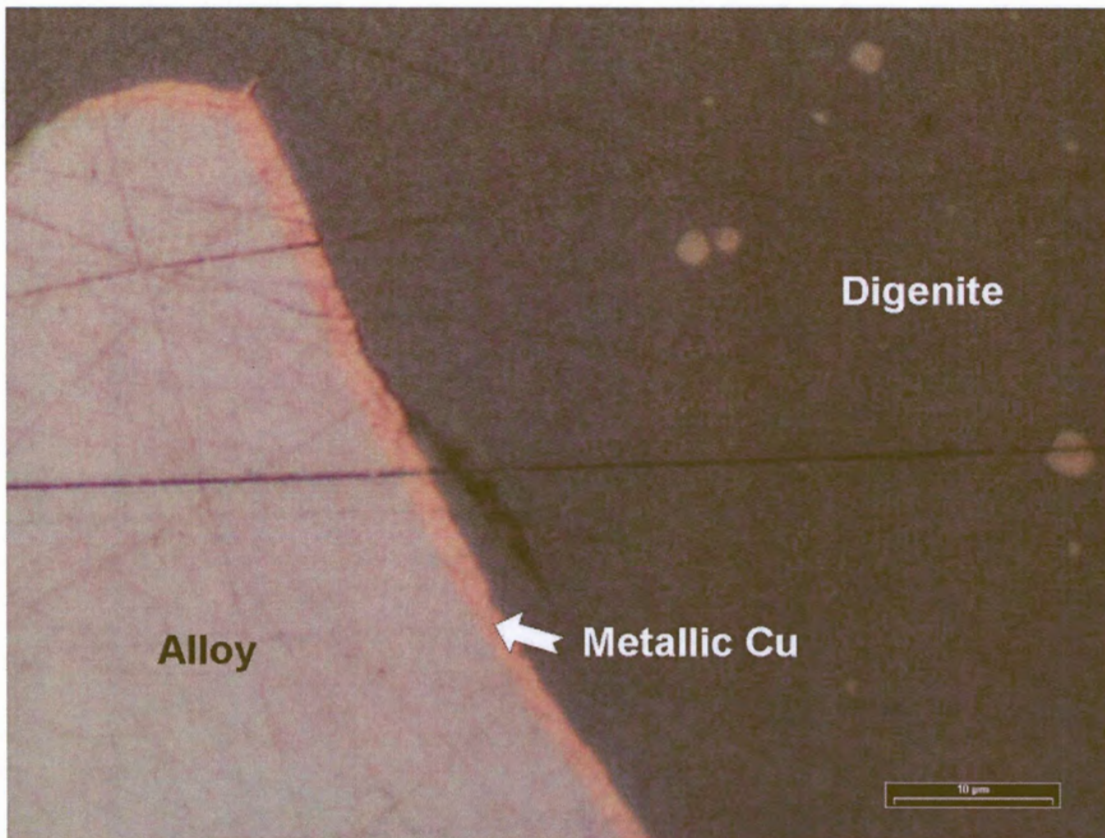
Photograph 5.2: Melt with euhedral alloy crystals (experiment 8a4).



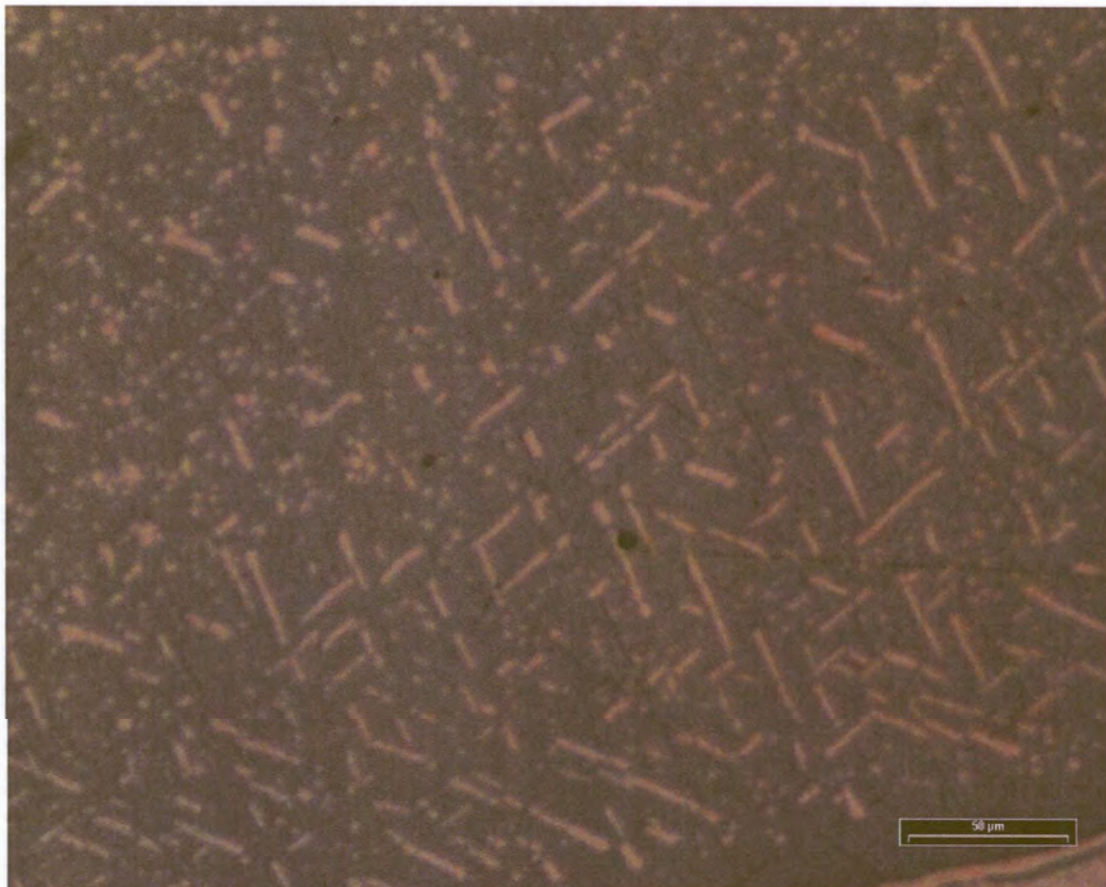
Photograph 5.3: Melt with skeletal alloy growths (experiment 10e1).



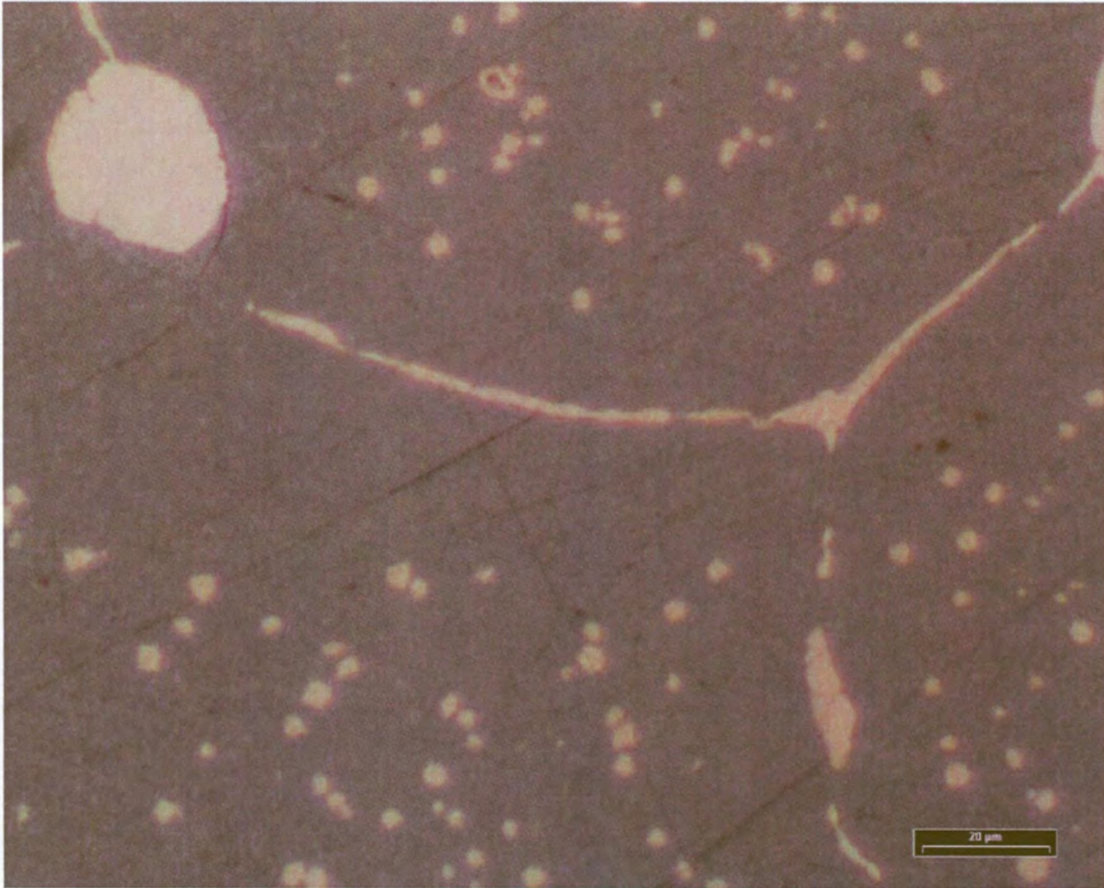
Photograph 5.4: Digenite crystals in melt with dendritic growth (experiment 10i3).



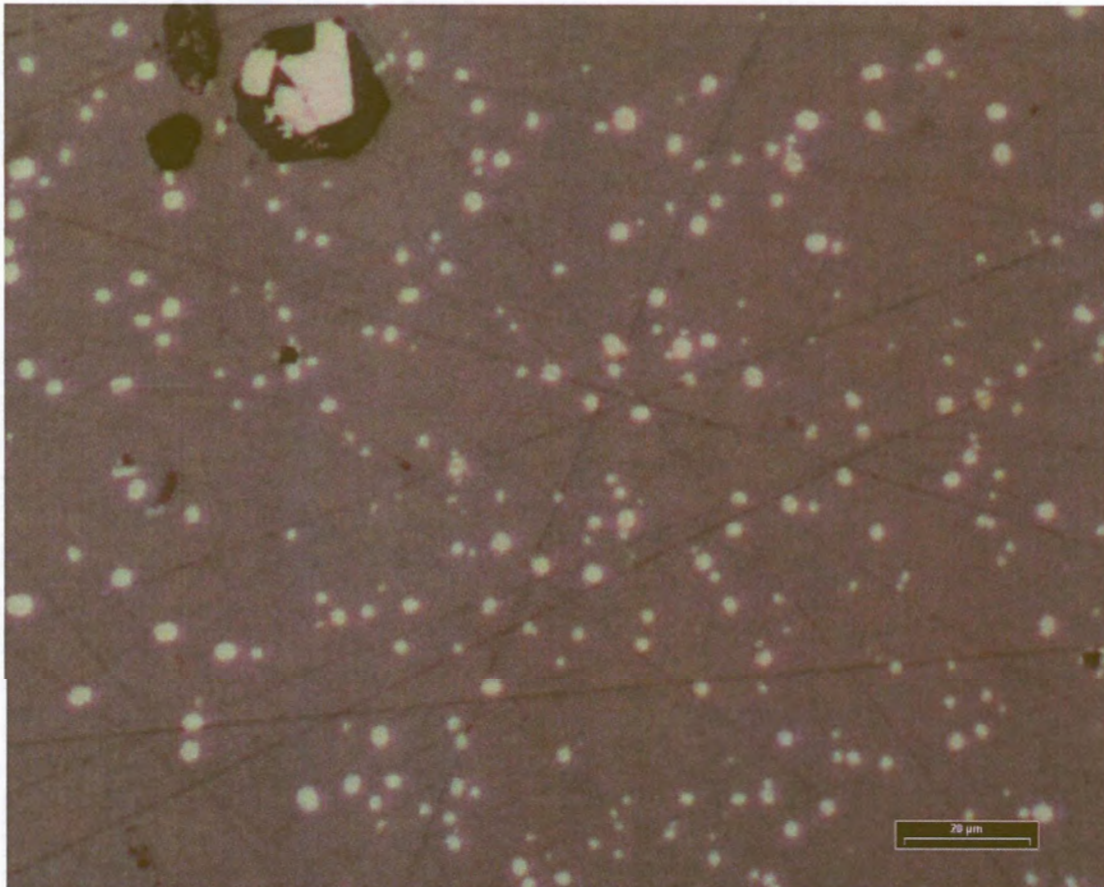
Photograph 5.5: Alloy and digenite with a rim of metallic copper (experiment 7e2).



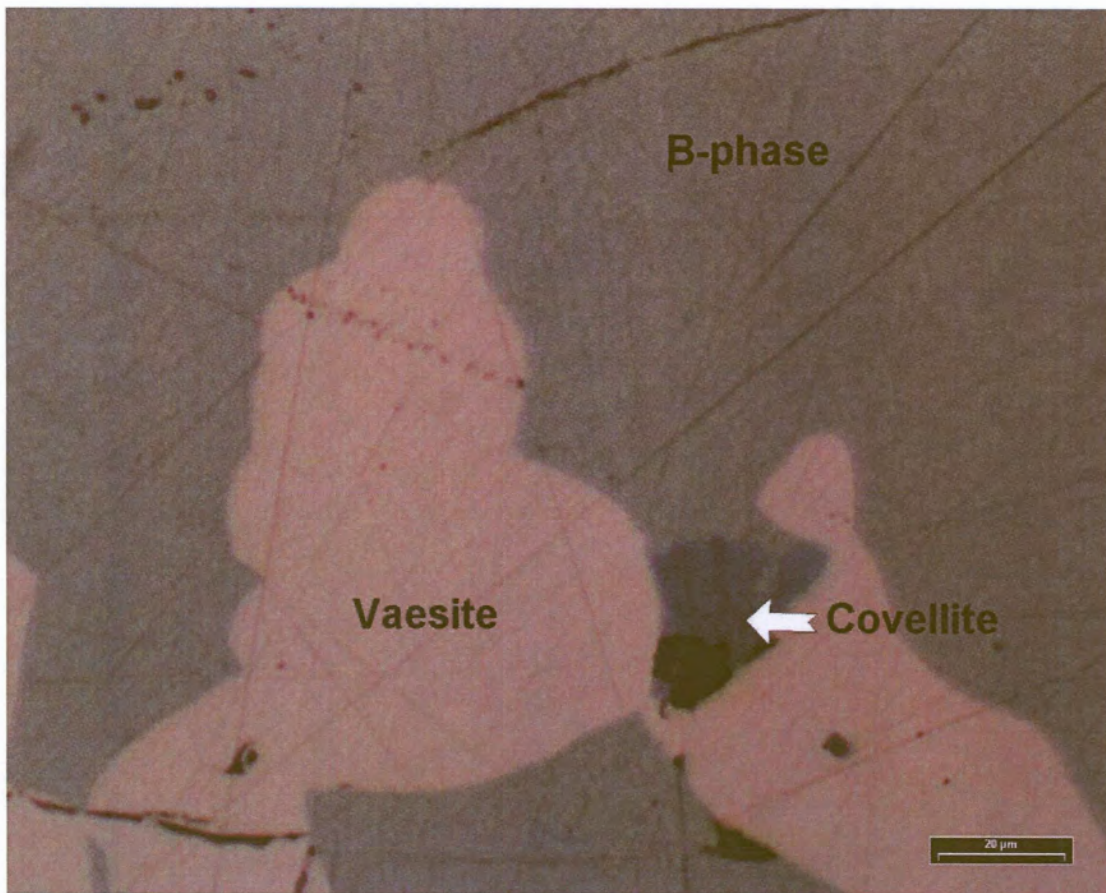
Photograph 5.6: Digenite with skeletal exsolutions (experiment 9e3).



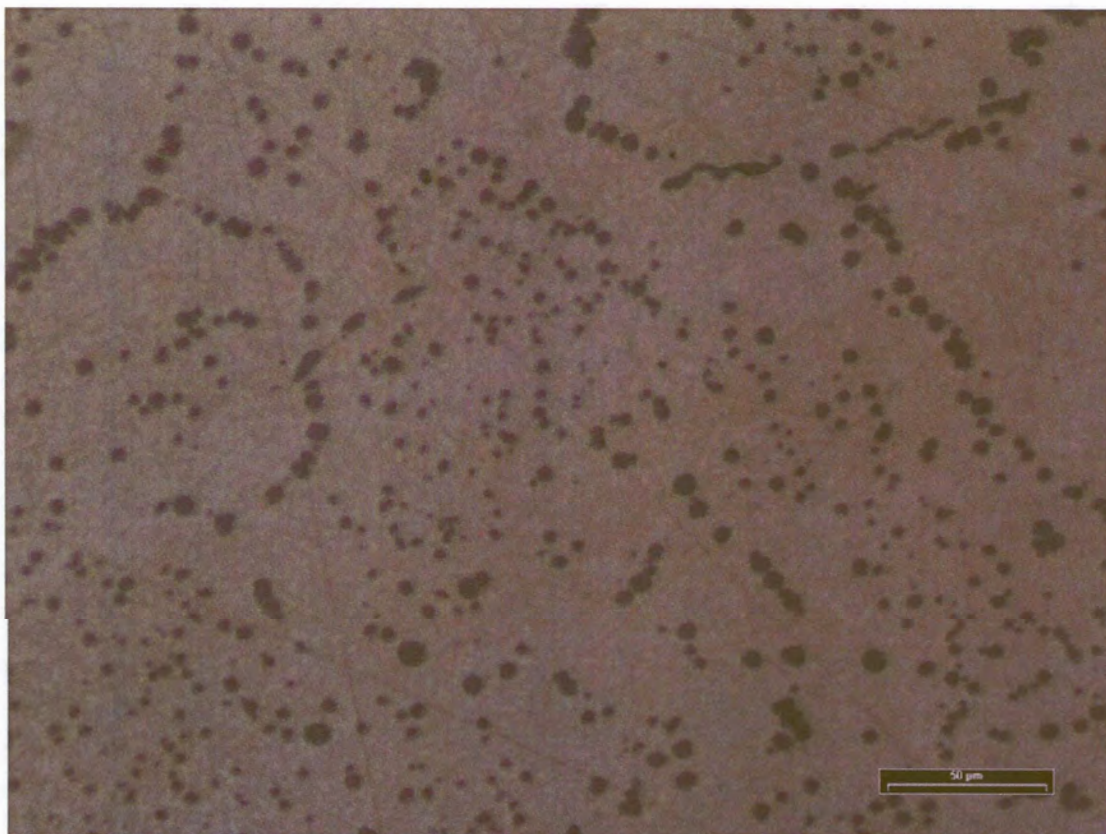
Photograph 5.7: Digenite with round exsolutions (experiment 9d4).



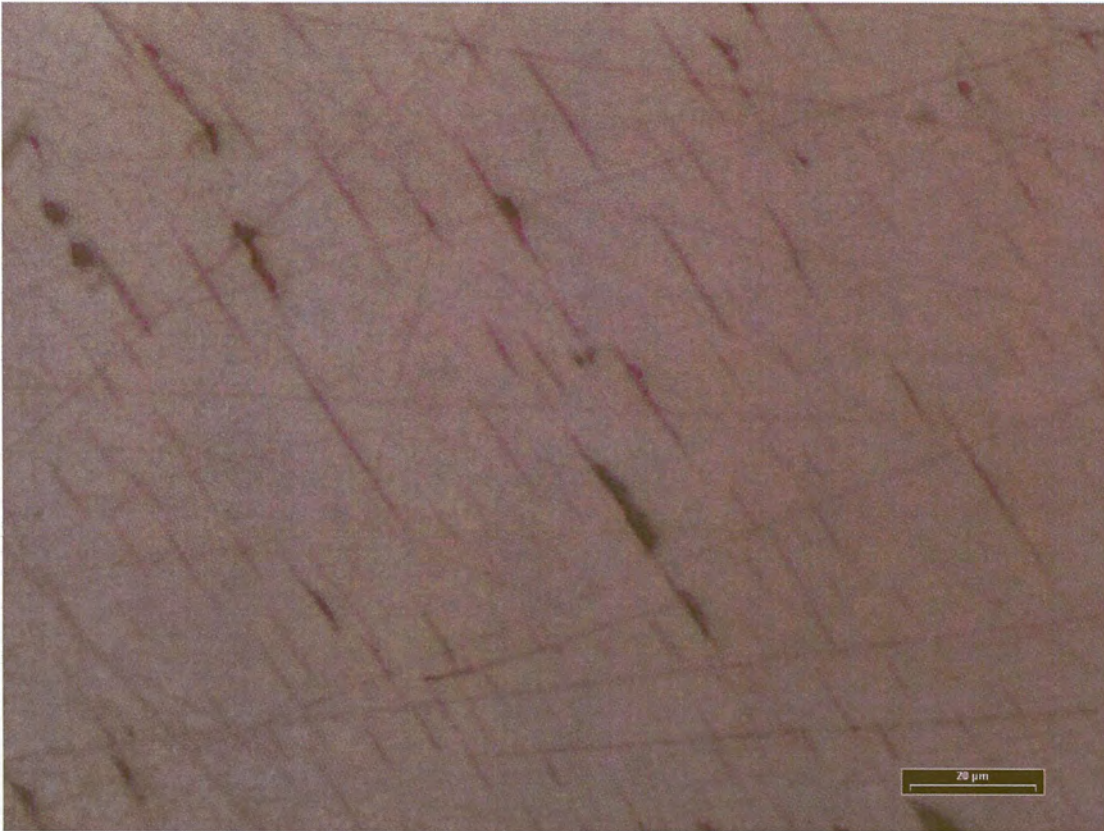
Photograph 5.8:  $\beta$ -phase with exsolutions of a Ni-sulphide (experiment 8m5).



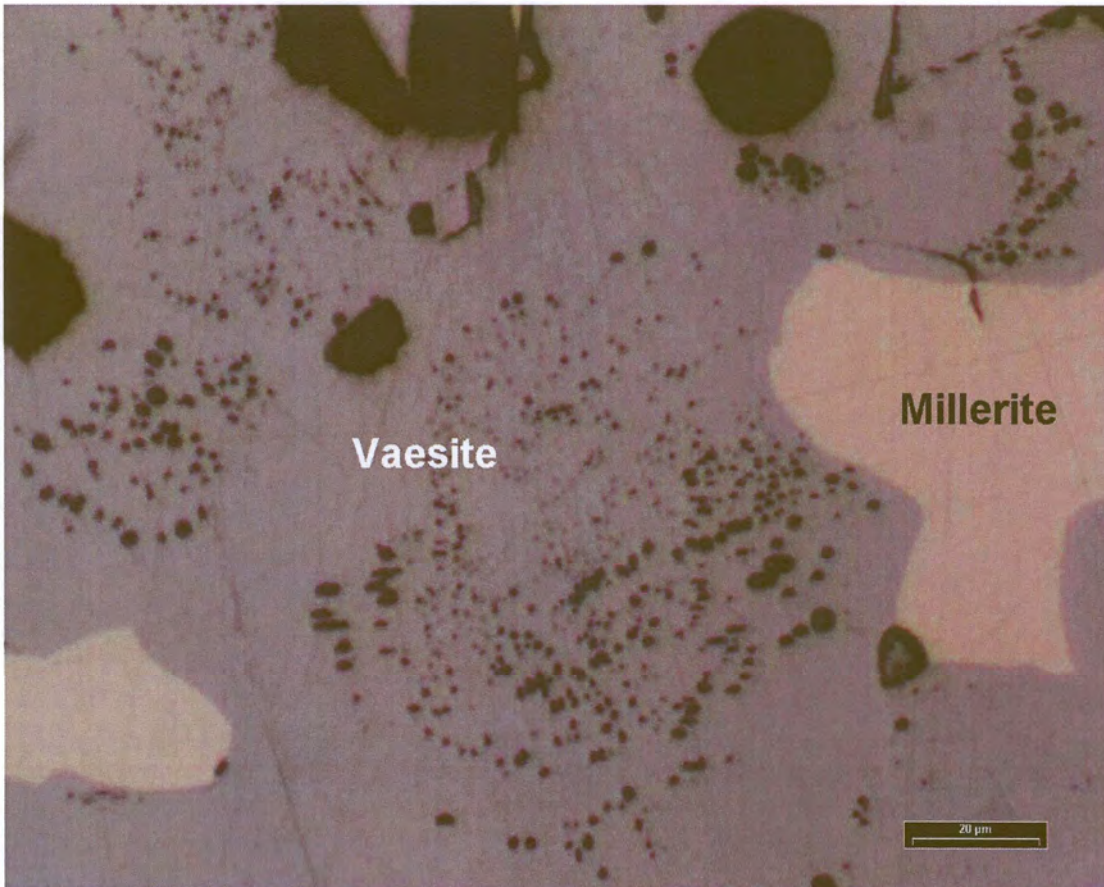
Photograph 5.9: Covellite associated with  $\beta$ -phase (experiment 7h4).



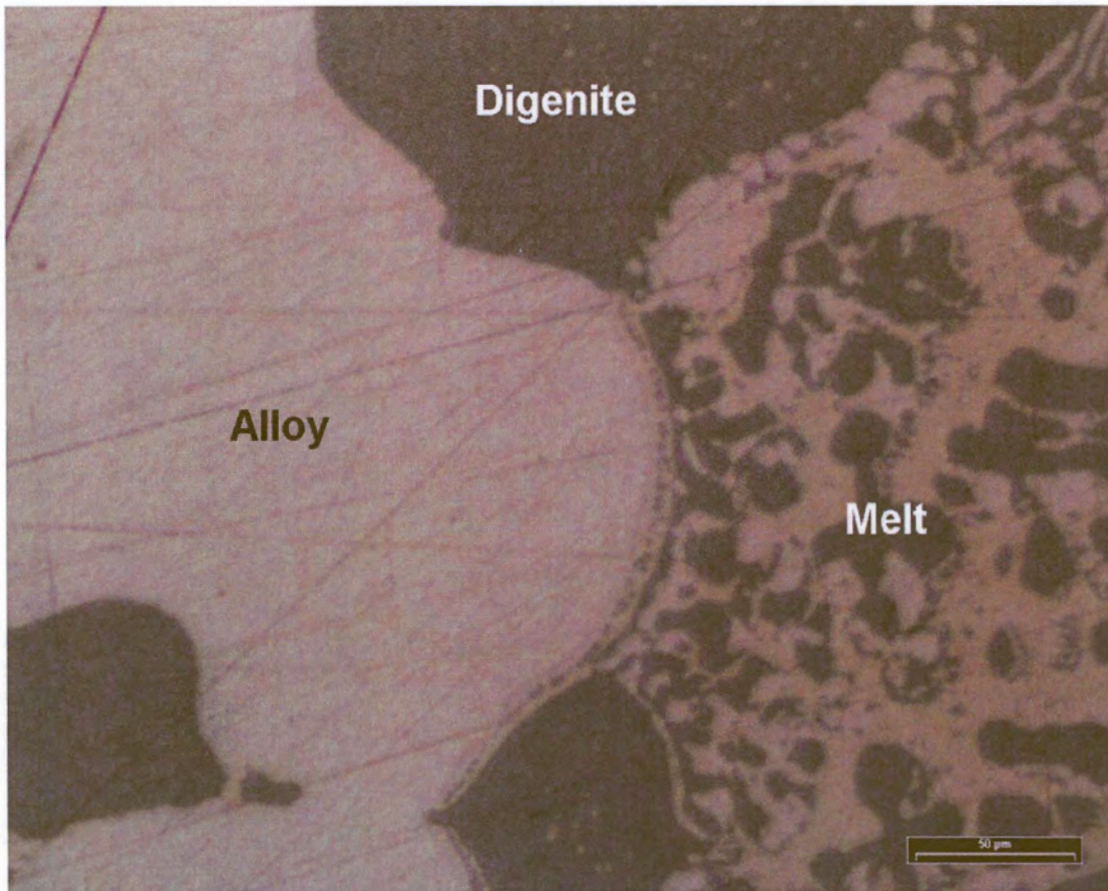
Photograph 5.10: Millerite with round exsolutions of a Cu-sulphide (experiment 8a1).



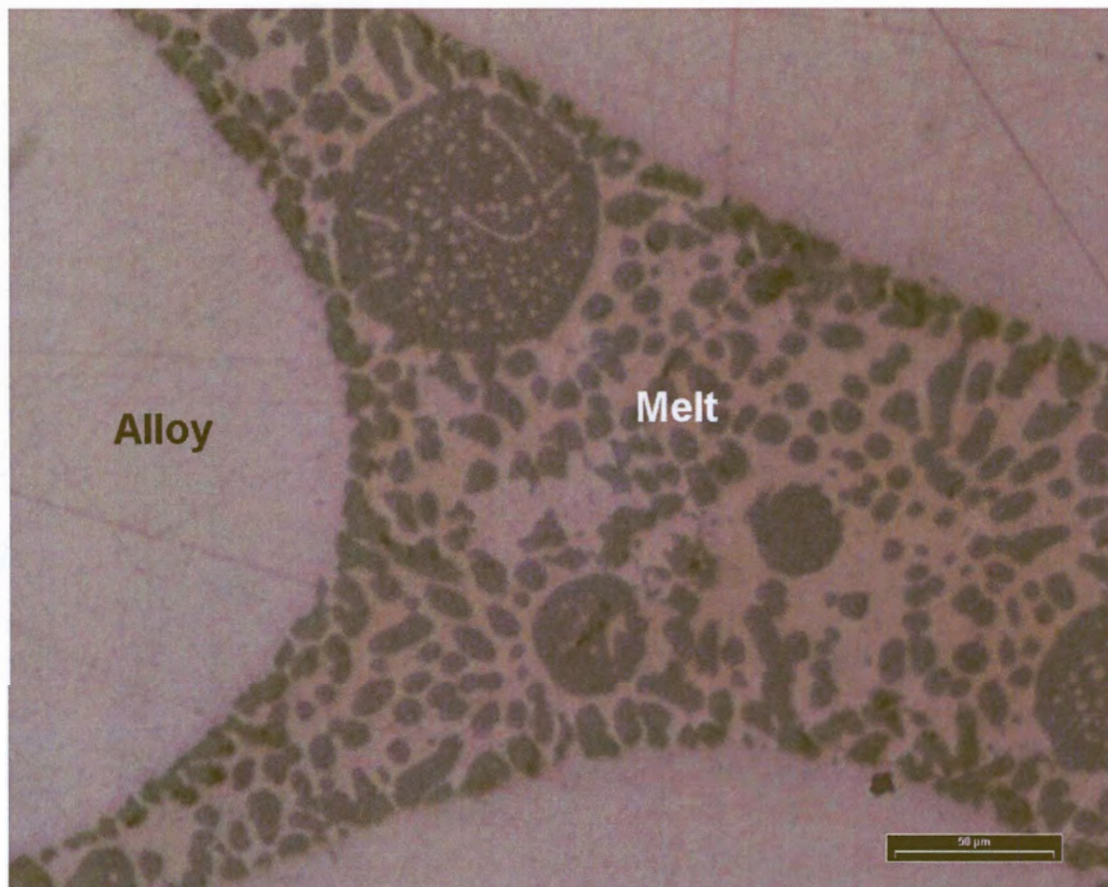
Photograph 5.11: Millerite with skeletal exsolutions (experiment 8m5).



Photograph 5.12: Vaesite with inclusions and associated millerite (experiment 8i4).

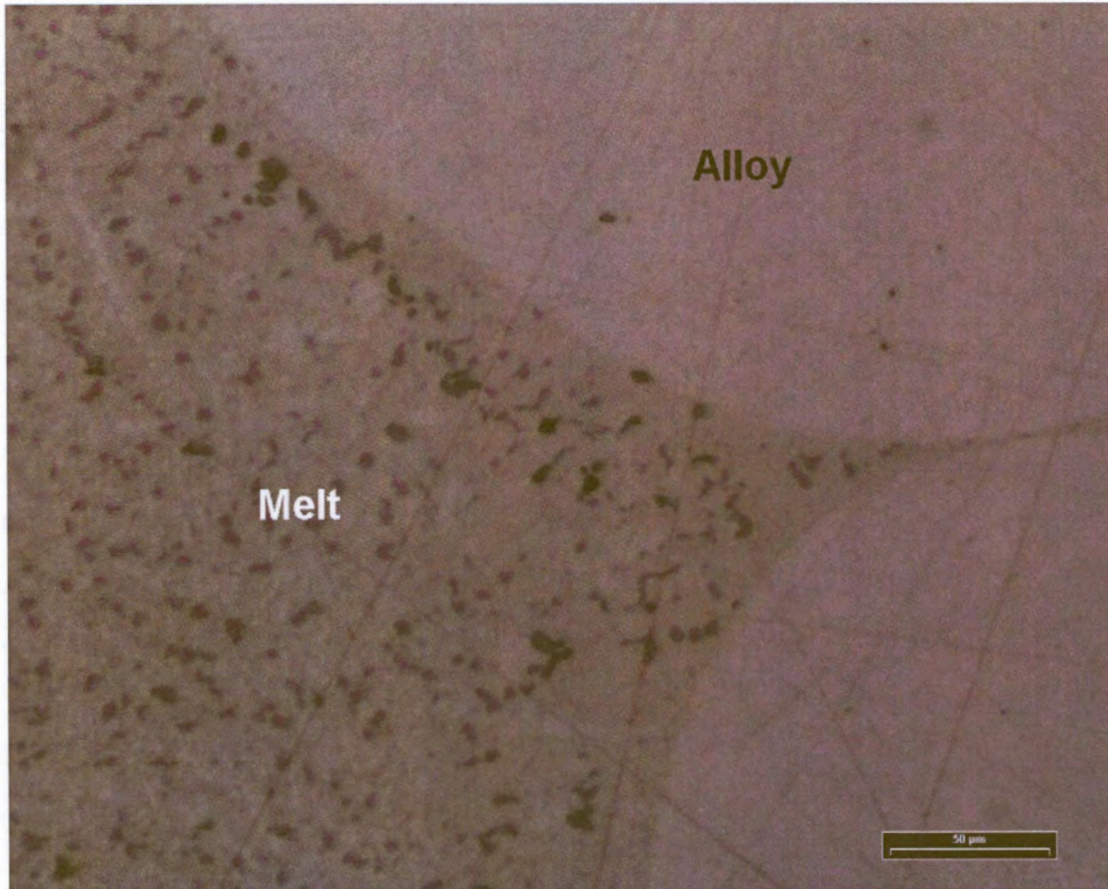


Photograph 5.13: Melt from the (alloy+digenite+melt)-assemblage(experiment 10j1).

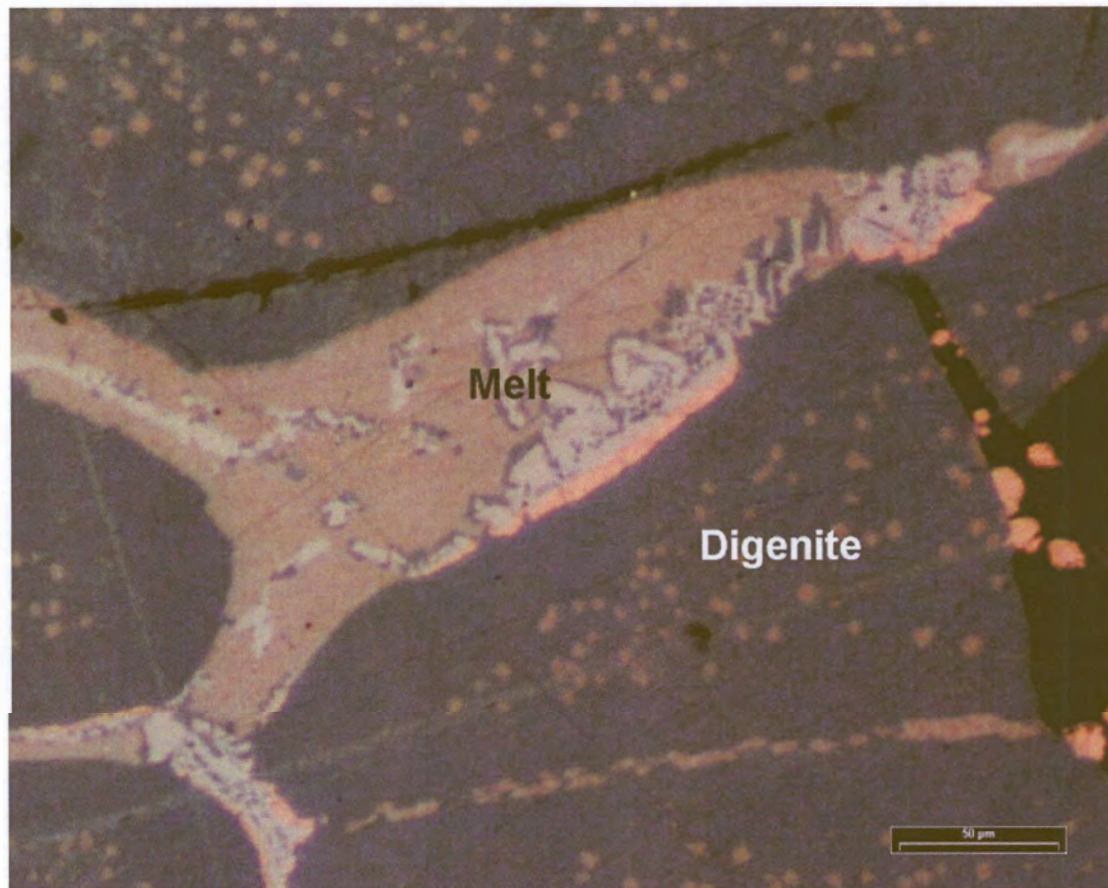


Photograph 5.14: Melt from a Cu-rich starting composition (experiment 10f4).





Photograph 5.15: Melt from a Ni-rich starting composition (experiment 8c5).



Photograph 5.16: Melt from a (digenite+melt)-assemblage (experiment 8d1).